TÜBİTAK

Turkish Journal of Earth Sciences

http://journals.tubitak.gov.tr/earth/

Research Article

Turkish J Earth Sci
(2023) 32: 330-350

doi:10.55730/1300-0985.1848

Geological structure informs rupture propagation and surface rupture complexity during the 2016 Kaikōura earthquake, New Zealand: insights for future large earthquake hazard

Kelvin BERRYMAN[1,*], Mark RATTENBURY[2], Stephen BANNISTER[2], Susan ELLIS[2], Pilar VILLAMOR[2], Donna EBERHART-PHILLIPS[3], Phaedra UPTON[2], Andrew HOWELL[2]

[1]Berryman Research & Consulting Ltd., Porirua, New Zealand
[2]GNS Science, Lower Hutt, New Zealand
[3]GNS Science, Dunedin, New Zealand

Received: 28.10.2022 • **Accepted/Published Online:** 19.12.2022 • **Final Version:** 28.04.2023

Abstract: We summarise the geological setting of complex surface rupture of the 2016 Mw 7.8 Kaikōura earthquake in the Marlborough Tectonic Domain of New Zealand. The event was complex both seismologically and geologically but not totally dissimilar to other large historical events globally. The earthquake occurred in the comprehensively imbricated, steeply-dipping Pahau Terrane crust that exhibits numerous tectonic overprints with diverse faulting styles. The current strike slip faults of the Marlborough Fault System are immature in their structural development and occupy, at least in part, inherited faults of earlier deformation phases. Several of the faults that ruptured in 2016 may connect at seismogenic depths. A listric fault geometry is likely for many of the faults that ruptured in 2016. This interpretation is supported by crustal seismic mapping identifying listric geometries for other large faults within the region. Examination of other historic surface rupturing earthquakes in the Marlborough Tectonic Domain and globally show some complexity but not to the same level of multifault rupture as in 2016. We conclude that multifault ruptures may be enhanced in the Kaikōura region where the Australian plate crust is thinner than farther west and the plate boundary deformation, at rates of >20 mm year^{-1}, transfers between closely-spaced faults with acute changes in surface geometry and with diverse rupture characteristics. The trend in seismic hazard assessment since 2016 is to include multifault ruptures universally, but this would be inconsistent with historic events in the Marlborough Tectonic Domain. Consideration of geological structure and history may usefully be incorporated into seismic hazard methodology to evaluate when and where multifault source models are indeed appropriate.

Key words: 2016 Kaikōura earthquake, surface rupture complexity, geological structure

1. Introduction

The 14th November 2016 Mw 7.8 Kaikōura earthquake is recognised as a very complex seismological and geological event in Marlborough, north-eastern South Island, New Zealand (Hamling et al., 2017; Kaiser et al., 2017; Litchfield et al., 2018, Hamling, 2019) (Figure 1). This region is in the transition zone from subduction at the Hikurangi margin along eastern North Island to a continental transform plate boundary in central South Island where approximately 80% of the relative motion is accommodated on the Alpine Fault (Howarth et al., 2018) (Figure 1). Strong motion in the 2016 had a duration of approximately 120 s and ruptures extended from the epicentre in north Canterbury (the eastern South Island) to the Needles Fault offshore of Cape Campbell over a distance of approximately 180 km (Hamling et al., 2017; Kaiser et al., 2017; Litchfield et al., 2018) (Figure 1). Aspects of the earthquake continue to be debated, particularly rupture complexity and rupture propagation (Ando & Kaneko, 2018; Ulrich et al., 2019; Chamberlain et al., 2021; Eberhart-Phillips et al., 2021a). Here, we address three of these aspects:

(i) The 2016 surface rupture complexity has been described as unprecedented and is increasingly informing future hazard, but several other historic fault ruptures have occurred in the region. We examine the complexity of those surface ruptures to consider whether the 2016 rupture was exceptional or similar to prior events. These events are the M7.6 Awatere Fault rupture in 1848, the M8.1 Wairarapa Fault rupture in 1855, the M7.1 Hope Fault rupture in 1888, and the M7.1 Poulter Fault rupture in 1929.

(ii) The factors that have contributed to the complexity of the 2016 surface ruptures, specifically how geological structure may have contributed to rupture complexity. We also investigate some global large earthquakes that were associated with variably complex surface ruptures and discuss possible drivers of complexity.

* Correspondence: kelvin@brc.nz

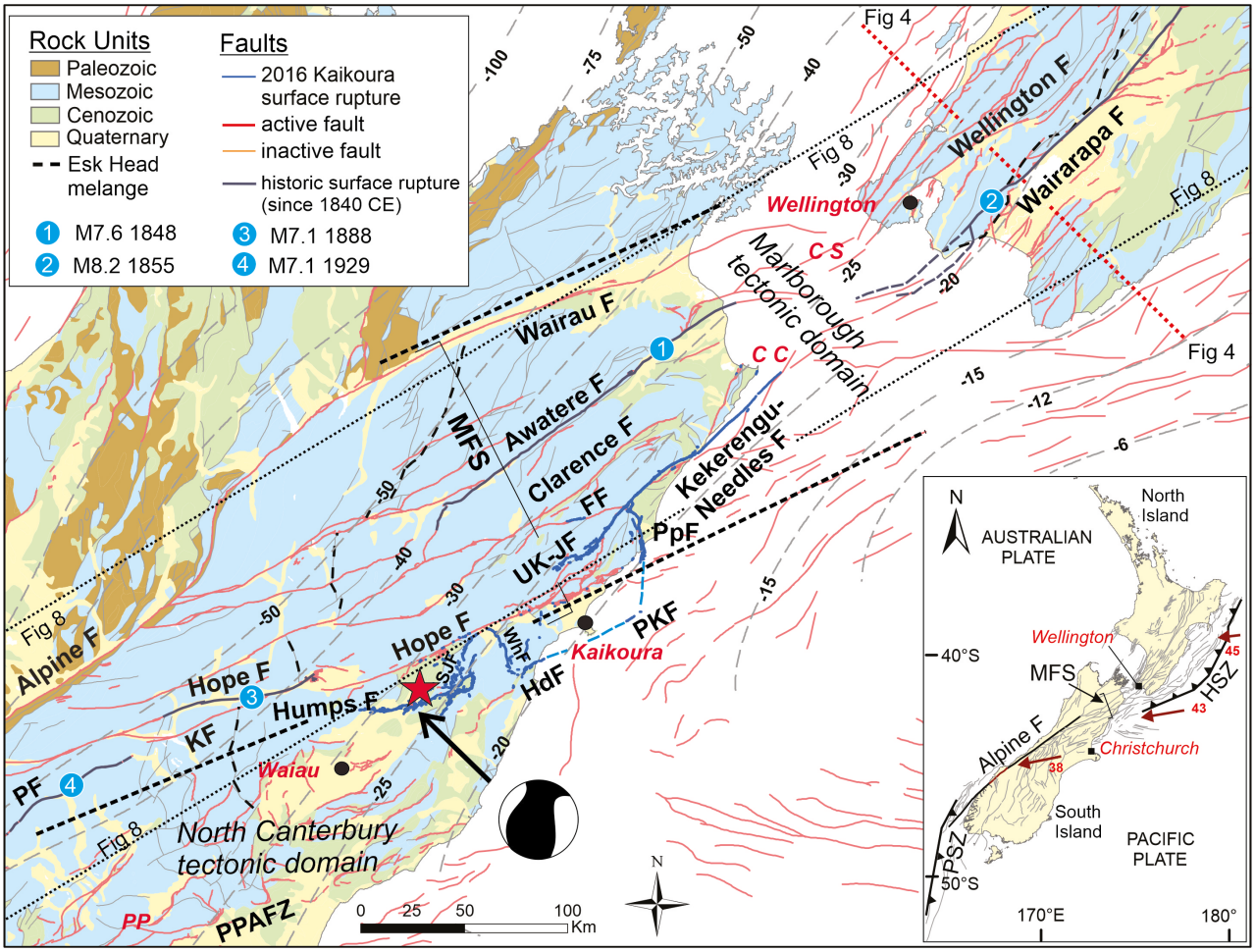

Figure 1. Generalised geological setting of central New Zealand showing the extent of the Torlesse terrane rocks and other units including the extent of the Esk Head Melange unit at the western boundary of the Pahau constituent of the Mesozoic Torlesse Terrane. Displacements across the strands of the Marlborough Fault System (MFS) indicate approximate total slip across the faults. Active faults (red) including: PPAFZ is Porters Pass-Amberley Fault Zone; PF is Poulter Fault; KF is Kakapo Fault. Faults that ruptured in the 2016 Kaikōura earthquake (blue) include: SJF is Stone Jug Fault; WhF is Whites Fault; HdF is Hundalee Fault; PKF is Point Kean Fault; UK-JF is Upper Kowhai-Jordan Fault; PpF is Papatea Fault. MFS is Marlborough fault system and spans the Wairau to Hope Faults. The extent of the Marlborough tectonic domain shown by dashed black lines and within that zone the extent of ruptures in the 1848 Awatere earthquake, 1855 Wairarapa earthquake, 1888 Hope Fault earthquake and the 1929 Poulter Fault earthquake are shown with blue circles and bold dark grey lines (Figure 8). Depth contours on the Hikurangi subduction interface beneath the North Island and the depth to the previously subducted oceanic crust in northeast South Island are shown as dashed grey lines with depths indicated. Geographic locations (red italics) include: CC is Cape Campbell; CS is Cook Strait; PP is Porters Pass. Red star shows the epicentre of the 2016 earthquake and the US Geological Survey dextral reverse focal mechanism. Location of cross section shown in Figure 4 is indicated by a dashed red line across southern North Island. Inset shows generalised plate boundary setting of New Zealand and regional active fault pattern with the MFS linking opposite dipping subduction zones, and the Alpine fault. Relative plate motion is shown (bold red arrows) with rates in mm year^{-1}.

(iii) We consider what future fault ruptures in the region might look like—similar multifault rupture complexity as in 2016 or simpler ruptures.

2. Tectonic setting and structural evolution of Marlborough

The transition zone in which the Kaikōura earthquake occurred is rapidly evolving (Cox and Sutherland, 2007) driven by oblique relative plate motion of approximately 43 mm year^{-1} near Cook Strait (Figure 1). The transition zone has been divided into two crustal tectonic domains in northeast South Island based on differing fault kinematics and fault slip rates (Pettinga et al., 2001; Stirling et al., 2012; Litchfield et al., 2014; Seebeck et al. 2022) (Figure 1). The domains arise partly because of the largely strike-slip Pliocene-Quaternary Marlborough Fault System (MFS) that overprinted bedrock structure related to subduction margin sedimentation and deformation of the bedrock in the late Jurassic to early Cretaceous (Ring et al., 2019) (Figure 1). Extensional tectonics then occurred

in the late Cretaceous. Contractional tectonics and crustal block rotation related to development of the present-day Australia-Pacific plate boundary occurred from the early Miocene (Little and Jones, 1998; Rattenbury et al., 2006) (Table 1). The relic Gondwana subducted oceanic slab underlies the Torlesse Terranes of Marlborough and north Canterbury forming a sharp rheological boundary (Eberhart-Phillips et al., 2021a).

2.1. Marlborough Fault System: inheritance can inform fault dip at depth

The Marlborough tectonic domain in northeast South Island is characterised by the four main elements of the MFS. These are the Wairau, Awatere, Clarence and Hope Faults (Figure 1). Near Kaikōura the majority of the slip rate of the Hope Fault transfers northward onto the shallow-dipping Jordan Fault, which is responsible for the uplift of the Seaward Kaikōura Mountains (Van Dissen and Yeats, 1991), and the Kekerengu-Needles Fault (Figure 1). An incipient new element of the MFS may be developing south of the Hope Fault; the Porters Pass–Amberley Fault Zone (Cowan et al., 1996; Howard et al., 2005) (PPAFZ on Figure 1). Inland, near Porters Pass (Figure 1) the PPAF is a dextral strike-slip fault. Further east, the deformation zone is less defined and broad with a series of overlapping asymmetric oblique reverse faults and folds involving the Tertiary cover strata. This characterises the North Canterbury tectonic domain where fault slip rates and strain rates are only approximately 10% of those in the Marlborough tectonic domain (Litchfield et al., 2003; Wallace et al., 2007; Litchfield et al., 2014; Seebeck et al., 2021).

Although the faults of the MFS have slip rates in the range of 4–20 mm year^{-1} (Litchfield et al., 2014; Seebeck et al., 2021), most are immature in terms of structural development resulting from their comparatively small total slip values and architecture of their surface rupture patterns. A useful piercing point across the MFS to illustrate the total dextral slip on the MFS is the Esk Head melange at the boundary between the Rakaia and Pahau greywacke bedrock terranes. Apparent total dextral offset of this piercing line is 90–100 km on the Wairau Fault, 12–14 km on the Awatere Fault, 16–18 km on the Clarence Fault, 16–18 km on the Hope Fault, and ≤8 km on the PPAFZ (Forsyth et al., 2008; Ghisetti, 2021) (Figure 1). Thus, only the Wairau Fault, as the northward continuation of the Alpine Fault, is likely to have a well-connected principal displacement zone. Ghisetti (2021) concludes that the strike-slip motion on the other Marlborough faults is younger than 5 Ma and less than 2 Ma for the Hope Fault.

In the Wairarapa region of southern North Island, Cashman et al. (1992) document the recent (probably <1 Ma) onset of strike-slip motion (with total slip of approximately 10 km) on the Wairarapa Fault (Figure 1), which overprinted a reverse fault regime that is well-exposed in the Pliocene-Quaternary sedimentary rocks through which the strike-slip fault is propagating. The recent strike-slip traces use suitably oriented parts of the reverse fault fabric but also break-through at slightly

Table 1. Tectonic history of Marlborough.

Age (Ma)	Episode	Characteristics in Marlborough	References
150–100	Gondwana margin subduction	Pahau Terrane sediments deposited and deformed in accretionary prism.	Rattenbury et al., 2006
		Esk Head melange developed as fault zone between accretionary prism and earlier accreted Rakaia Terrane	Ring et al., 2019
105–60	Breakup of Gondwana & opening of Tasman Sea	Extension - widespread erosion, normal faulting and sedimentary basins formed	Bradshaw, 1989 Crampton et al., 2003
60–35	Passive margin	Mild extension – deposition of widespread carbonate rocks	Crampton et al., 2003 Landis et al., 2008
35–25	Convergence in early phase of current plate boundary	Uplift of Inland Kaikōura mountains and reverse faults in parts of the region	Rait et al., 2001 Collett et al., 2019
25–8	Hikurangi subduction	Convergence across many Marlborough fault including	Little & Jones, 1998
	margin fully developed	ancestral MFS, dramatic vertical axis rotations	Randall et al., 2011
8–0	Plate re-organisation with more convergence at Alpine Fault	Southern Alps uplift & progressive development of MFS	Batt et al., 2004 Ghisetti, 2021

different locations in the near-surface (Lamarche et al., 2005). Thus, the strike-slip faults of Marlborough (with the exception of the Wairau Fault) and southern North Island are all likely to have locally complex surface rupture patterns as a result of their immaturity (Wesnousky, 1988; Milliner et al., 2016; Hutchison et al., 2020; Goldberg et al., 2020).

2.2. Crustal structure from geological mapping: inferences of fault geometry at depth

None of the studies following the Kaikōura earthquake have directly imaged fault rupture planes at depth. However, surface observations of the structural geology of the basement terrane in which the 2016 Kaikōura earthquake occurred helps to make sense of the complex rupture dynamics and complicated surface deformation pattern related to the earthquake. These data have not, until now, been considered but are important and overlooked aspects in understanding the likely geometry of the faults that ruptured and how they may be connected at depth. All the 2016 Kaikōura earthquake surface ruptures occurred within the late Jurassic-early Cretaceous Pahau Terrane, a constituent unit of Torlesse Terrane in the northern South Island (Mortimer et al., 2014; Edbrooke et al., 2014) (Figure 2). The Pahau Terrane consists of low-grade zeolite and prehnite-pumpellyite facies greywacke. These rocks are commonly well-bedded with generally steep dips (median 68°, Edbrooke et al., 2014) and generally steeper (median 75°) transposed or foliated zones (Figure 3).

The metamorphic grade of the Pahau Terrane represents a maximum crustal thickness or burial depth of approximately 15 km (assuming upper bound temperature and pressure conditions of around 350 °C and 6 kbar pressure) (Bishop, 1972). However, the predominantly steeply-dipping Pahau Terrane extends across-strike a minimum surface distance of 80 km (Figure 2) without concomitant metamorphic grade change. This implies that the Pahau Terrane has been comprehensively imbricated. That is, the width of the zone of relatively constant metamorphic grade has increased through multikilometre displacements on what are today often a north-striking network of reverse faults. These faults produced stacked, rotated slices of the upper crust Pahau Terrane (Figure 2). The area depicted in the inset of Figure 2 has a particularly high density of such faults. We expect the higher density in this area is a function of exposure and field mapping and that a similar density of faulting occurs throughout the Pahau Terrane. The depths of the putative decollement surfaces in the modern setting are not well constrained but based on the homogeneity of metamorphic grade and recognition that the structures initially developed in a low-angle accretionary prism subduction margin setting with listric reverse faulting (Ring et al., 2019) then the geometry of the Pahau Terrane faults is probably much like those in the present-day Hikurangi subduction margin (Barnes et al., 2002; Bailleul et al., 2013). Modern listric faults in the Hikurangi subduction margin typically flatten at depths of 6–12 km (Bailleul et al., 2013; McArthur et al., 2020) and this is likely to be the case for the initial Pahau Terrane faults that have been steepened by shortening, extended during the late Cretaceous and again shortened and rotated during Cenozoic deformation (Table 1). Thus, the preponderance of steep faults observed at the surface in the Kaikōura region probably do not persist deeper than midcrustal depths of 6–12 km. The orientation and attitude of these legacy Mesozoic north-striking faults are well-oriented for reactivation as oblique reverse faults in the current stress field. The Papatea Fault (Figures 1 and 2) which ruptured in the Kaikōura earthquake with up to 12 m of reverse-sinistral displacement (Langridge et al., 2018) is one of these structures.

The older history of the Papatea Fault has been documented by Lensen (1962) and Rattenbury et al. (2006) showing Pahau greywacke thrust over late Cretaceous and Paleogene sediments. Langridge et al. (2018) and Diederichs et al. (2019) determine a minimum near-surface dip of 50°W but the broad uplift pattern associated with the approximately 15 km wide Papatea block in the 2016 earthquake (Zinke et al., 2019) may indicate that the fault shallows with depth, although the uplift pattern may also be influenced by possible near-shore faults adjacent to the Papatea block (Howell and Clark, 2022). Similarly, the broad uplift patterns associated with the Humps East and North Leader Faults, and potentially the Whites Fault, in the North Canterbury Tectonic Domain (see Figure 1 for locations) near the earthquake epicentre (Nicol et al., 2018; Zinke et al., 2019) are also suggestive of shallowing of surface fault dip with depth. However, while it is plausible that these N-S striking faults have a shallower dip at depth, it is hard to constrain their geometry using available geodetic and seismological data. It is especially hard to separate the effects of slip on these N-S striking faults from those with slip on SW-NE-trending faults like the Hundalee Fault (Williams et al., 2018) and the fault that uplifted the Kaikōura Peninsula in 2016 (Clark et al., 2017; Mouslopoulou et al., 2019).

The question of dip on the MFS faults at seismogenic depth is informed by consideration of how strike-slip faulting might overprint preexisting structure in the Pahau greywacke as discussed above and is also informed by structural style in north Canterbury in general proximity of the PPAFZ where the strike-slip overprint is incipient. Structural geology studies in the North Canterbury domain identify oblique slip on predominantly N-NE oriented listric reverse faults (Litchfield et al., 2003). Farther south, in south Canterbury, listric structure has also been interpreted (Long et al., 2003; Stahl, 2014). We should therefore presume this geometry was also typical of Marlborough before the recent overprint of strike-slip deformation became developed. Shallowly-dipping

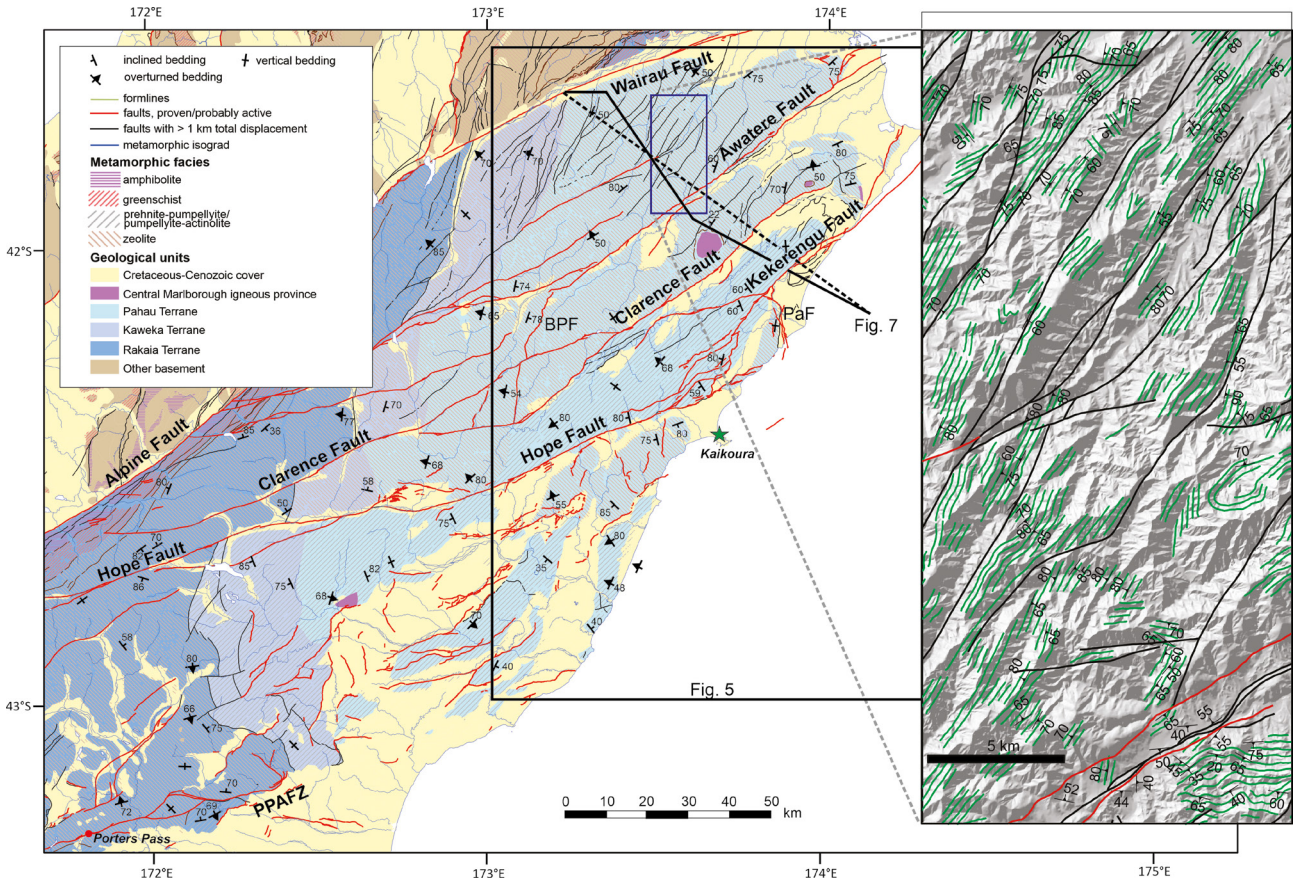

Figure 2. Geological map of northeast South Island showing extent of the Pahau and other terranes, their metamorphic grades, large-displacement bedrock faults, active faults, including Barefell Pass Fault; PaF = Papatea Fault. The map area of Figure 5 and crosssection locations of Figure 7 (solid line is the geological cross section and dashed line is the Vp and Qp geological transect) are also shown. Inset illustrates aspects of the detailed structure in the Pahau Terrane with steep, generally NNE-striking surface faults, NE striking active strike slip faults (red) and widespread steep to overturned bedding in the Pahau rocks shown by formlines and structural measurement data. Adapted and summarised from Rattenbury et al. (2006) and Edbrooke et al. (2014).

fault planes at seismogenic depth are therefore likely on the deep portions of the MFS. Similarly shallow-dipping portions of the older Mesozoic reverse faults are potential linking structures on which the 2016 earthquake may have propagated between the principal faults. A seismic reflection profile across southern North Island imaged the deeper part of the Wairarapa Fault and has been interpreted to have a listric geometry (Henrys et al., 2013) suggesting continued occupation of the older geometry of a subduction margin reverse fault (Figure 4). A listric geometry or rupture of a low angle deep fault is also required to fit the uplift distribution of the 1855 earthquake across southern North Island (Darby and Beanland, 1992; Beavan and Darby, 2005).

2.3. Regional geophysics: imaging rheology and gross structure

In addition to the surface geology, interpretations of crustal structure inferred from passive-source seismic data (Eberhart-Philips & Bannister 2010; Ellis et al., 2017) also provide insight into crustal structure, rock types and rheology at seismogenic depths in northeast South Island. Mapping of the position of the plate interface (Williams et al., 2013): thinning of the overlying plate to the southeast and the depth to a constant P-wave velocity (and iso-velocity depth map) provide useful insight into geological structure in the upper crust. High P-wave velocities in the upper crust (V_p > 6.2 km s^{-1}) are interpreted as greenschist facies schist, basalt, and ultramafic rocks which are not observed at the surface (Ellis et al., 2017). Vp gradients are prominent in proximity to some of the currently active faults in Marlborough, with the isovelocity depth for V_p = 6.2 km^{-1} varying from <7.5 km to >25 km depth (Figure 5). Shallow blocks of $V_p \geq 6.2$ km^{-1} such as to the west of the present-day Awatere Fault (Figure 6) are inferred to be primarily related to the presence of schist or perhaps exotic blocks from the Pacific oceanic crust transferred to the

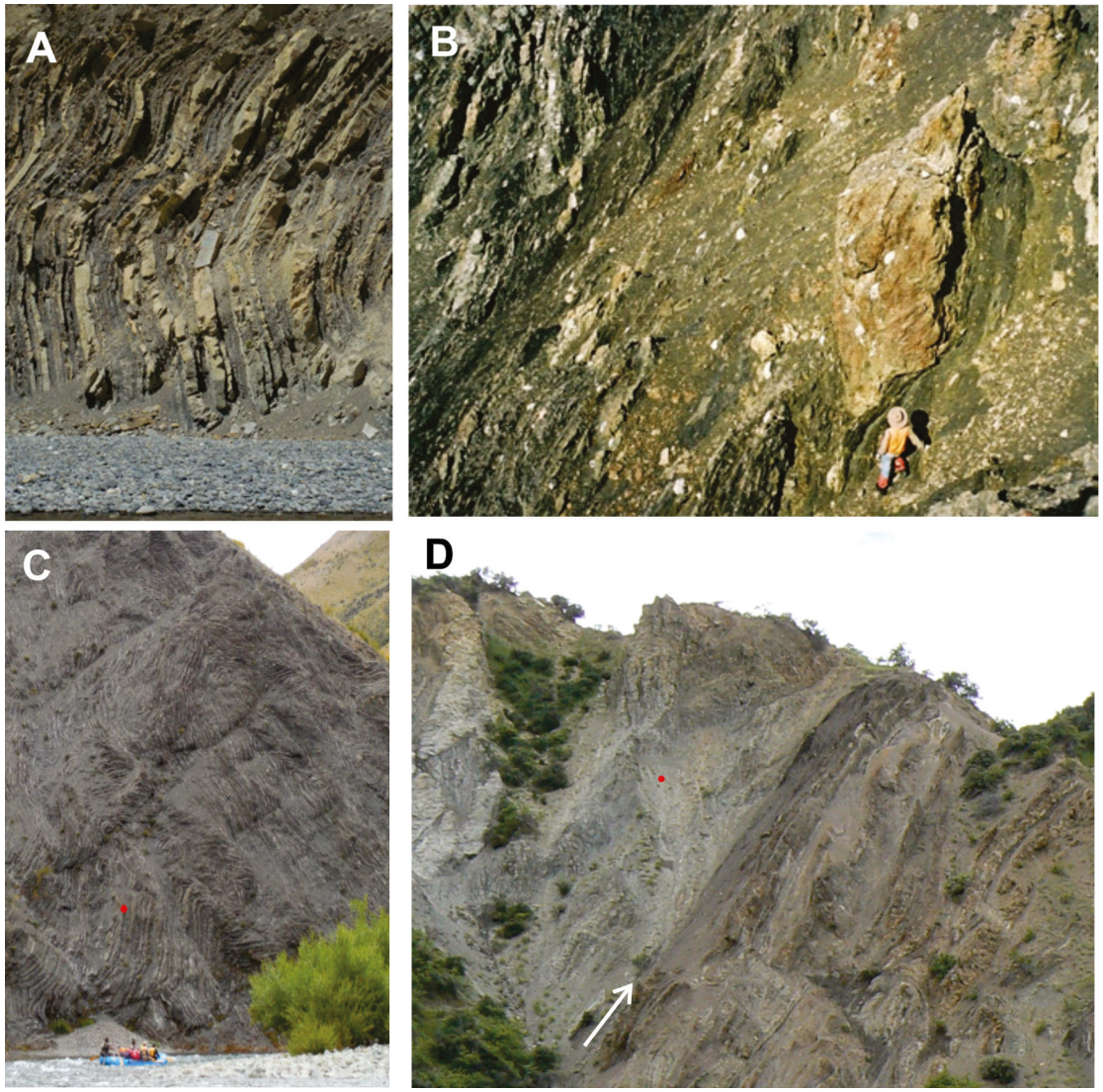

Figure 3. Field photographs of typical constituents of Pahau Terrane greywacke. A. Well-bedded, steeply-dipping alternating sandstone and mudstone in the middle Clarence valley. B. Melange zone in the Seaward Kaikōura Range. C. Folded bedding in thinly alternating sandstone and mudstone. Photos: M R Johnston and M Rattenbury D. Re-activated high angle fault with grey gouge cutting Pahau Terrane greywacke in middle Clarence Valley (shown by arrow).

Australian plate during Mesozoic subduction, supporting the interpretation that there are major fault structures in the shallow crust that only partly coincide with the present-day active faults. We note that the predominant strike-slip motion on the MFS cannot be responsible for the large differences in depth of this Vp iso-contour, and instead point to pre-MFS displacement on older structures in the Torlesse bedrock of the region, consistent with interpretations of surface geology.

3. Rupture complexity in the 2016 earthquake

The spatial extent and characteristics of surface faulting in 2016 has been extensively documented (Clark et al., 2017; Stirling et al., 2017; Kearse et al., 2018; Langridge et al., 2018; Little et al., 2018; Litchfield et al., 2018; Nicol et al., 2018; Williams et al., 2018). To the south of the Hope Fault the surface ruptures were typically characterized by short (≤3–4 km) en-echelon or branching segments separated by gaps or step-overs. These form a complex array of dextral-oblique, reverse, and sinistral-slip ruptures (Nicol et al., 2018; Williams et al., 2018). In contrast, surface fault ruptures to the north of the Hope Fault comprise a nearly continuous zone of surface fault rupture over a cumulative strike length of approximately 87 km (Figure 1). The entirety of the previously mapped onshore Kekerengu Fault (approximately 27 km) ruptured along with approximately

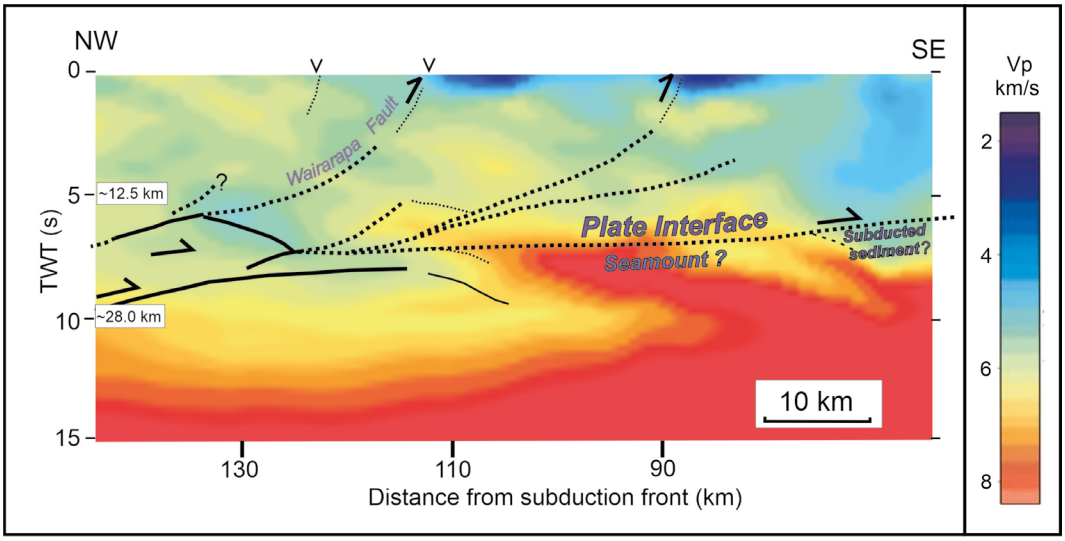

Figure 4. Interpreted crustal reflections in a transect across southern North Island (Henrys et al., 2013) showing possible listric structure of the Wairarapa Fault (dotted black line) soling onto an underplated ramp duplex. Other velocity irregularities near the plate interface are interpreted as subducted seamount material (high velocity) and underplated sediments (low velocity patch). Interpretation of the subduction interface position is from Williams et al. (2013).

30 km of the offshore Needles Fault zone and 30 km of the onshore Jordan Fault, Upper Kowhai and Manakau Faults (Figure 1). This northern domain also includes surface fault rupture on the north-northwest-striking Papatea Fault (Langridge et al., 2018) and the northeast-striking Fidget Fault (Figure 1). Triggered slip on two segments of the Hope Fault were also recorded and short ruptures with up to 1.5 m slip occurred southwest of the Papatea Fault as well as west of the Needles Fault near Cape Campbell (Litchfield et al., 2018).

In terms of the rupture sequence, the earthquake initiated on The Humps Fault, about 10 km northwest of the Hundalee Fault strand of the PPAFZ (Nicol et al., 2018) (Figure 1). The rupture then moved to a series of generally northeast-striking dextral-reverse faults, including partial rupture of the Hundalee Fault (Williams et al., 2018) and its likely offshore extension (Clark et al., 2017), as well as more northerly-striking sinistral-reverse faults. Rupture of the Whites Fault extends to within a few kilometres of the Hope Fault and only 2–3 km from large displacement ruptures on the Snowflake Spur strand of the Upper Kowhai-Jordan-Kekerengu-Needles Fault (Howell et al., 2019; Zinke et al., 2019). Surprisingly, given the high slip rate of the Hope Fault and its prominence in the kinematics of the MFS, it did not have significant surface rupture in 2016. At the surface, only short discontinuous surface ruptures were observed (Litchfield et al., 2018), consistent with triggered slip rather than primary ruptures.

The propagation of rupture from the North Canterbury domain to the Marlborough domain has been inferred to be largely the consequence of dynamic triggering 'jumping across' the Hope Fault (Ando and Kaneko, 2018) or a more continuous linkage from the north Canterbury faults to the Hundalee Fault south of Kaikōura Peninsula, linking to an offshore section of the Papatea Fault (or proposed Offshore Splay Thrust Fault of Nicol et al., 2022) and then to the Jordan-Kekerengu-Needles Faults (Chamberlain et al., 2021). In the 2016 earthquake, the Jordan Fault ruptured with a component of dextral-normal displacement in contrast to the long-term reverse motion (Van Dissen & Yeats, 1991). Moreover, the Papatea Fault had a significant sinistral component of motion in the 2016 earthquake (Langridge et al., 2018; Diederichs et al., 2019), but exposures of the western strand fault plane on the shoreline at Waipapa Bay also had a set of striae with a steep southeast plunge consistent with dextral motion in an earlier event. Therefore, we might expect that some of the faults that enable the transfer of motion from the Hope Fault to the Kekerengu Fault may have different rupture kinematics depending on the rupture propagation and participation of the Hope Fault. Kinematically, the transfer of slip from the Hope Fault to the Kekerengu Fault via the Jordan Fault would most likely involve reverse motion on the Jordan Fault and perhaps reverse-dextral motion on the Papatea Fault.

A recent review of the surface deformation data from GPS, InSAR, and optical satellite images (Hamling, 2019) and inversions of the data highlights the diversity of fault source models as well as the ongoing debate as to whether the Hikurangi subduction interface ruptured coseismically

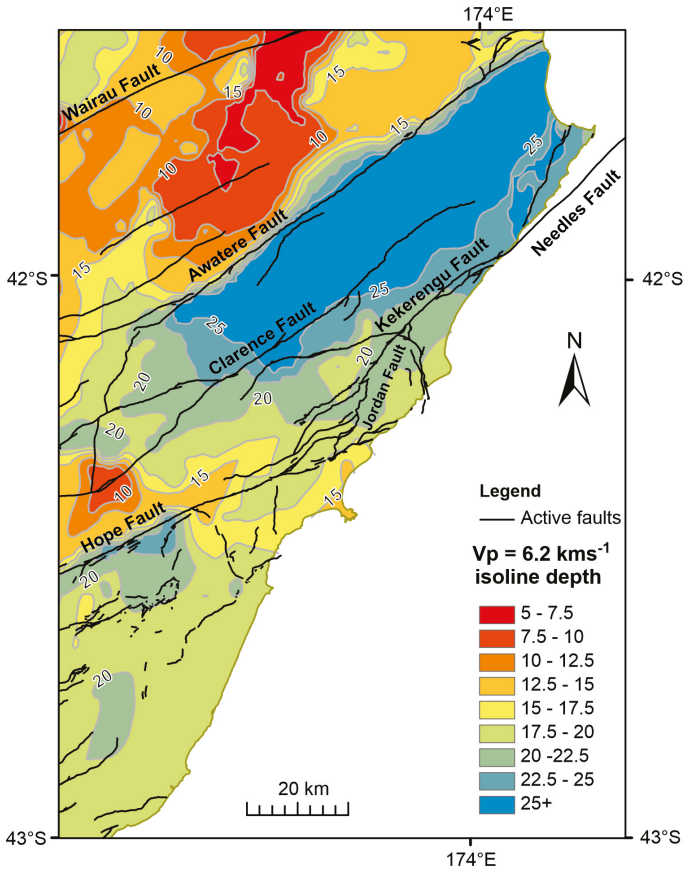

Figure 5. Map of Vp > 6.2 km^{-1} contours (approximating the depth to greenschist facies and other high velocity rocks) in northeast South Island in relation to contemporary active faults (area shown in Figure 2). The steep gradient is prominent near the Awatere Fault, but the apparent 'displacement' is far too great to be associated with the strike-slip active fault which has only 15–20 km of total slip. Steep gradients in other locations are suggestive of relict structure and/or related to listric faulting and deeper shear zones beneath the MFS (based on Eberhart-Phillips et al., 2010). Across the faults at the surface, there is a consistent uniform metamorphic grade in the Pahau Terrane greywacke rocks.

in the Kaikōura earthquake. Readers are referred to the recent review (Hamling, 2019) for detailed discussion of the fault source inversion studies and discrepancies, but in summary Hamling considered that much of the uncertainty comes from the lack of resolving power of the surface deformation and teleseismic data and the diversity of methods used to infer slip at depth. Any deformation caused by slip at depth is swamped by the large ground displacements from the shallower sources, making interpretation of the coseismic slip distribution at depth highly nonunique (Xu et al., 2018).

4. Focal mechanisms and aftershocks

The global seismic moment tensor indicated a composite dextral-reverse fault with one of the nodal planes, oriented NNE, consistent with average surface fault orientations and dominant structural grain of the region (Figure 6). The majority of aftershocks are ≤18 km depth (Lanza et al., 2019; Chamberlain et al., 2021) apparently several kilometres above the depth to the subducted oceanic crust which is about 20 km below surface beneath the Kaikōura coast, 25–27 km below the surface near the epicentre of the mainshock, and 30 km beneath the Clarence Fault (Williams et al., 2013) (Figures 1 and 7). Active subduction begins in Cook Strait, and there eight aftershocks have been associated with the subduction interface at 26–28 km depth. Several authors (Cesca et al., 2017; Lanza et al., 2019) note the clustering of aftershock seismicity in the midcrust and aftershock activity between the spatially distinct surface faults with a variety of focal mechanisms, which is consistent with the presence of complex linkages between faults in the upper brittle crust, as can be inferred from structural geology data. Aftershock locations are quite diffuse and tend to be to the north or west of the surface traces of faults, indicative of north or westward dip on the faults at mid crustal depths. A number of features in the seismicity such as the Snowgrass Creek Fault (Chamberlain et al., 2021) (Figure

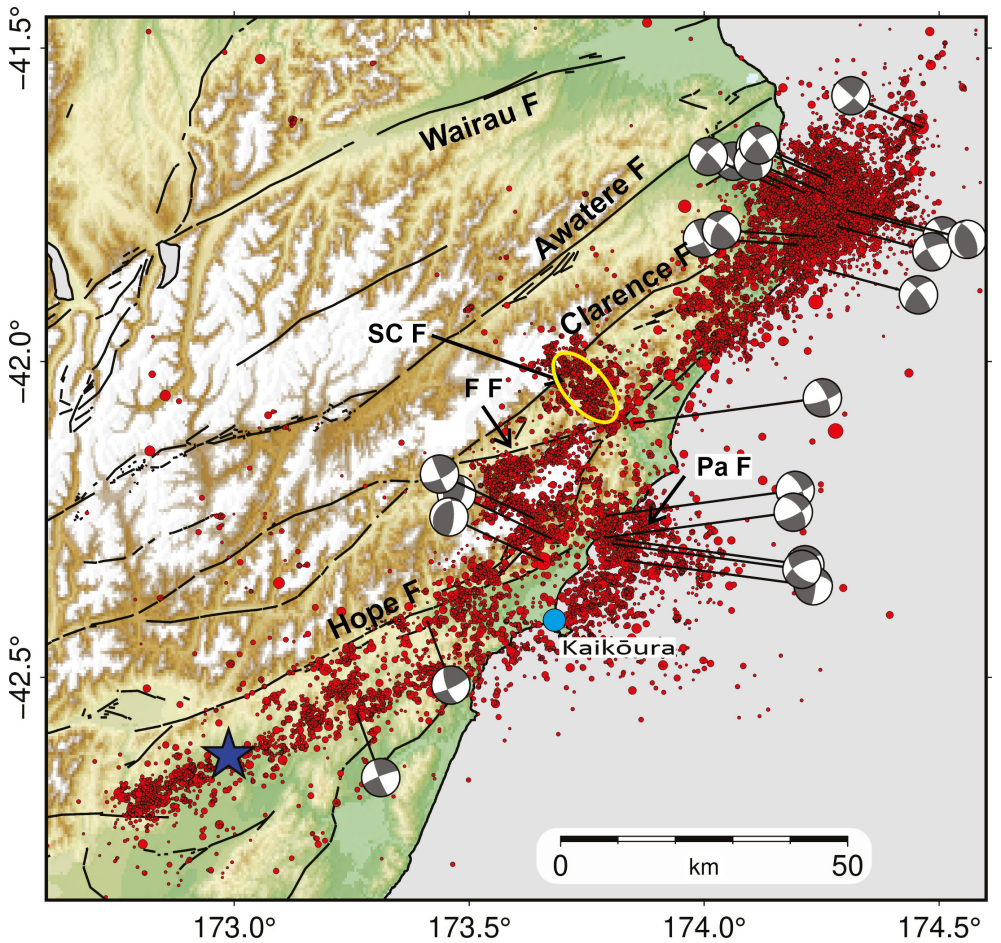

Figure 6. Aftershock locations from Chamberlain et al. (2021) for all events with magnitudes >1.0. Source mechanisms from Cesca et al. (2016) for events with magnitude >5. Blue star shows the epicentre of the initial mainshock. F F is Fidget Fault; Pa F is Papatea Fault; SC F is Snowgrass Creek Fault (cluster of aftershocks shown by yellow ellipse).

6); have no surface expression but are suggestive of linkage at depth. Elsewhere, concentrations of aftershocks indicate areas of high stress such as in the area around the Papatea and Fidget Faults. At the northeast end of the rupture the intense cluster of aftershocks is associated with rupture termination.

In Figure 7, we plot the inferred structure to 5 km depth from surface geology (Figure 7a) and geophysical data (p-wave velocities (Vp, Figure 7b) and the inverse of p-wave seismic attenuation (Qp, Figure 7c). Vp depends on rock properties, particularly density (e.g., Christensen and Mooney, 1995). In the brittle crust, Q also depends on rock properties (rocks with a high elastic strength have higher Q) but is also sensitive to rock damage (fracturing). In ductile crust, Q can be reduced by grain-boundary sliding and thus outline areas of ductile deformation. Eberhart-Philips et al. (2021b) interpreted the region of low Qp (≤400) at 25–30 km depth (Figure 7c) in terms of ductilely deforming lower crust. The largest afterslip occurred in a shallowly-dipping zone (Wallace et al., 2018) in the low Qp region downdip of the Kekerengu Fault rupture, which is consistent with afterslip occurring downdip of large earthquakes in zones where long-term creep may also occur that loads the base of crustal faults (Eberhart-Phillips et al., 2021b). Aftershocks are concentrated within a region of low Qp in the brittle crust, interpreted to represent enhanced fracturing and fluid-related deformation (Figure 7c). This anomaly is also seen in Vp but not so prominently (Figure 7b). The anomaly is bounded to the east by a region of normal Qp > 600 at approximately 15 km depth, indicative of less rock deformation in this area than further west. These interpretations from seismic tomography (Figures 7b and 7c; Eberhart-Phillips et al., 2014, 2021b) are consistent with the proposed listric fault model inferred from surface mapping and geological history.

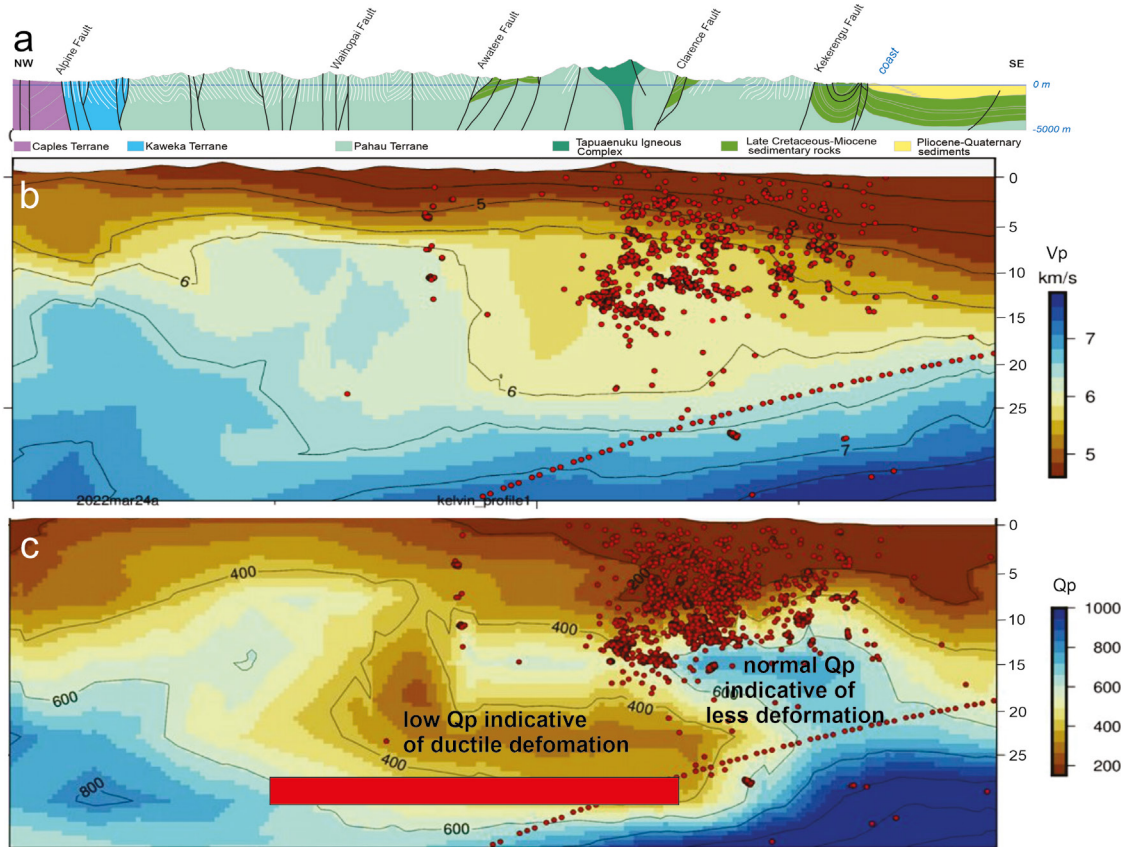

Figure 7. Cross section of (a) geological cross section from Rattenbury et al. (2006) (b) P-wave velocity (km s^{-1}): (c) Qp (1/attenuation). Location of the NW-SE profile-lines are shown in Figure 2. Seismicity locations are from Chamberlain et al. (2021), projecting event hypocentres within ±8 km either side of the profile line. P-wave velocities and attenuation models are from Eberhart-Phillips et al. (2021a, 2021b). Dashed red line shows the depth of the Hikurangi plate interface model from Williams et al (2013). Red bar on Qp section shows horizontal extent of afterslip associated with the 2016 earthquake (from Wallace et al., 2018)

5. Surface rupture complexity in historical earthquakes in the Marlborough tectonic domain

In this section, we ask the question as to whether other large earthquakes with accompanying surface rupture in the Marlborough tectonic domain (MTD) were similarly complex like the 2016 Kaikōura event. We restrict the time period to since widespread European settlement of New Zealand in about 1840 when diaries of early landowners provided first-hand accounts and were, in some cases followed-up with contemporary scientific field studies (e.g., McKay, 1890). We also include the 1855 Wairarapa Fault rupture in this assessment because it lies in an analogous structural setting as the defined MTD.

The potential to discern historical rupture complexity is impacted by the tools and data available to researchers in the aftermath of the event. Following the 14 November 2016 earthquake, the immediate field-based studies did not have access to modern remote sensing data and the reconnaissance (albeit using extensive helicopter support) had established, approximately 3 weeks after the earthquake, there had been rupture on nine faults. Over the following months, a further 12 faults were detected, some by continued field studies, but many were detected by analysis of remote sensing data (Howell et al., 2019; Zinke et al., 2019). These new techniques began to be used for fault rupture studies from about 2002 (Hudnut et al., 2002; Zinke et al., 2019). The additional fault ruptures associated with the 2016 earthquake, detected from remote sensing, had <2 m maximum displacement (Litchfield et al., 2018) and often <1m. Thus, we may presume that a proportion (perhaps up to 50%) of surface rupture may be missing from historical (prior to 2000 CE) surface rupture mapping studies, but most of these will likely to have had displacements of <2 m. There are exceptions to the completeness of early studies depending on aerial photograph coverage and terrain. For example, fault ruptures associated with the 1992 Landers earthquake in the Mojave Desert of California were mapped to a high

level of completeness with centimetre resolution (e.g., McGill and Rubin, 1999).

Therefore, when we interpret the degree of complexity of surface rupture associated with historic earthquakes in the MTD, we acknowledge there was likely to be additional ruptures of subsidiary faults and there was likely to be more diffuse deformation along the principal ruptures. The question as to whether the intensity of deformation of the bedrock in the MTD varies and is at least partly responsible for observed variation in rupture complexity in recent earthquakes also needs consideration. At present, geological mapping suggests the Pahau Terrane rocks of the MTD are similarly deformed across the region although the timing of uplift and geomorphic development across the region varies (Collet et al., 2019; Ghisetti, 2021).

5.1. 1848 M7.6 Awatere Fault (Figure 8C)

Grapes and Downes (1997) reviewed the historical data on the large earthquake that occurred early in history of European settlement in New Zealand. The fault ruptured from White Bluffs on the coast (where dextral displacement of 3.7 m was recorded 300 m inland) to near Molesworth. Mason and Little (2006) undertook a detailed survey of the smallest offsets observable along the fault, interpreting these as 1848 displacements. At the inland end of the rupture near Molesworth, the 1848 rupture appears not to have followed the Molesworth section of the fault but ruptured at least some of the Barefell Pass Fault (BPF) where Mason and Little (2006) identified a 4.8 ± 1.2 m dextral displacement of a small stream channel at Barefell Pass (Figure 1 and Table 2). The horizontal slip

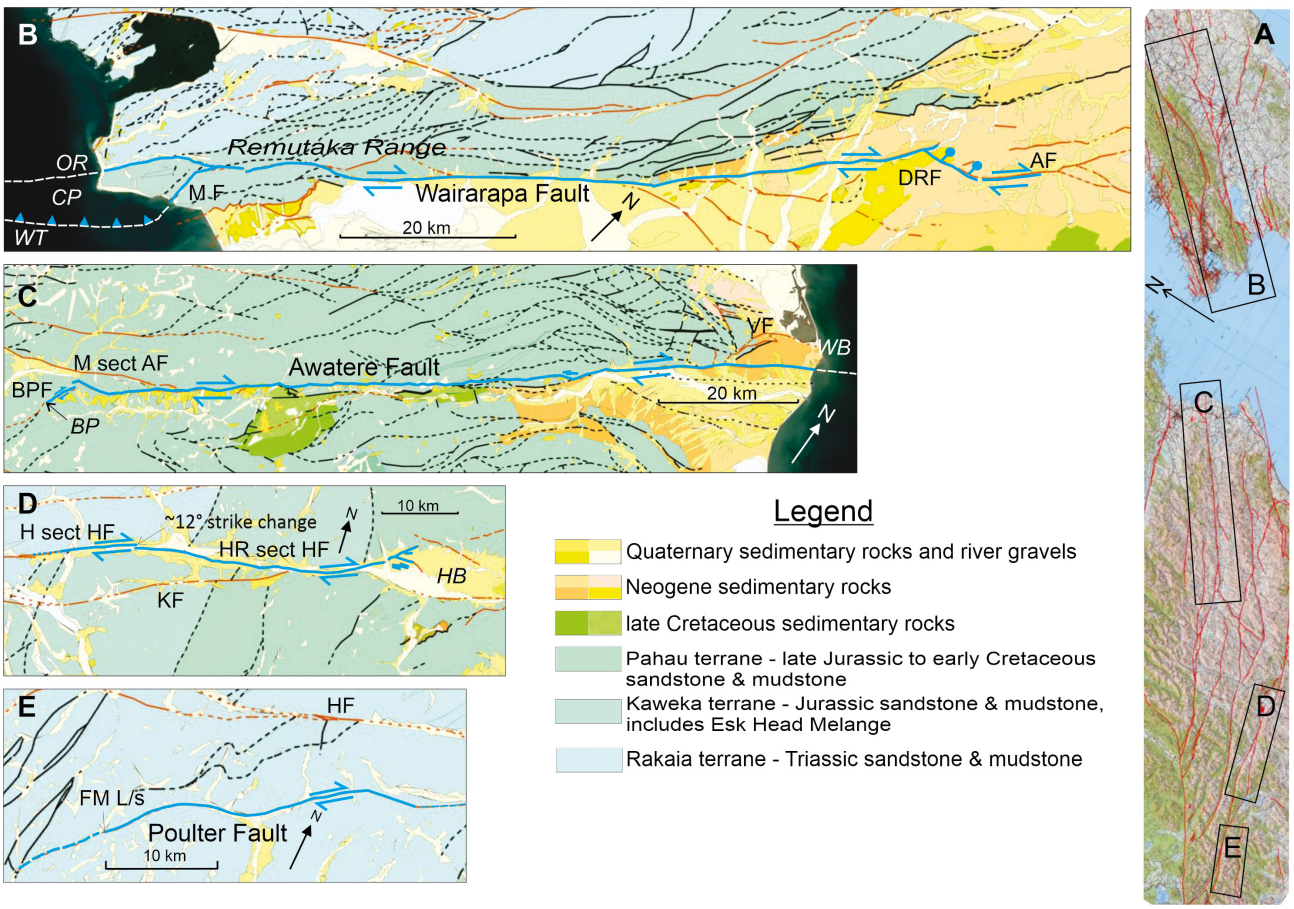

Figure 8. Surface fault ruptures associated with recent historical earthquakes (post-1840 CE) in the Marlborough tectonic domain. Geological units are from the online 1:250,000 scale geological map of New Zealand (last accessed May 2022). A - Reference map showing the areas covered by individual events. B - 1855 Wairarapa Fault earthquake (AF is Alfredton Fault; CP is Cape Palliser; DRF is Dreyers Road Fault; MF is Mukamuka Fault; OR shows location of Orongorongo River mouth; WT is Wharekahau Thrust). C - 1848 Awatere Fault earthquake (BP shows location of Barefell Pass; BPF is Barefell Pass Fault; M sect AF is Molesworth section of Awatere Fault; VF is Vernon Fault; WB shows location of White Bluffs). D - 1888 Hope Fault (Amuri) earthquake (HB is Hanmer basin; H set HF is Hurunui section of the Hope Fault; HR sect HF is Hope River section of the Hope Fault; KF is Kakapo Fault). E. 1929 Poulter Fault (Arthur's Pass) earthquake (FM L/S shows location of Falling Mountain landslide; HF is Hope Fault).

Table 2. Characteristics of some earthquakes with complex surface rupture and historic earthquakes in the Marlborough tectonic domain.

Name	EQ Mag.	Fault Slip Rate (mm year^{-1})	Date	Tectonic setting	Predominant displacement	Nature of complexity	Number of faults	Total sfc fault length (km)
Gobi-Altai, Mongolia	8	0.5–1.0 [1]	1957	CI	sinstral strike-slip	Multifault, multiple fault types, ruptures up to 25 km apart	6	~300
Landers, USA	7.1	0.4–0.7 [2]	1992	PBr	dextral strike-slip	Multifault with 1–3 km step-overs with linkage ruptures between faults	6	95
İzmit/Düzce	7.4/7.1	18–25	1999	PB	dextral strike-slip	Multiple geometric segments, secondary normal faults	1	145/35
Denali, Alaska, USA	7.9	8–12 [3]	2002	PB	dextral strike-slip	Multifault, multiple fault types, end-on ruptures	3	330
El Mayor-Cucupah, Mexico	7.2	2–5 [4]	2010	PBr	dextral normal	Multistrand of complex fault, several parallel ruptures	1	60
Darfield, New Zealand	7.1	0.04–0.06 [5]	2010	PBr	dextral strike-slip	Multisegment at surface but 6 faults in the subsurface	1	28
Ridgecrest,	7.1 (6.4 f/s*)	<<0.7 [6]	2019	PBr	both dextral & sinistral strike-slip	Multifault, orthogonal ruptures. Mainshock followed 34 h later	2	55
Awatere	7.6	4–8 [7]	1848	PBr	dextral strike-slip	Possible 2 fault rupture with initial rupture of the Barefell Pass Fault	2	>110
Wairarapa	8.2	8–12 [7]	1855	PBr	dextral strike-slip	6 km step-over and partial rupture of Alfredton Fault at north end. Probable slip partitioning on Wharekahau Thrust and strike-slip section at southern end	2	~150
Hope	7.1	11–17 [7]	1888	PBr	dextral strike-slip	Ruptured through a geometric segment boundary along-strike	1	~45
Poulter	7.1	0.5–1.7 [7]	1929	PBr	dextral strike-slip	None observed	1	~36
Kaikōura	7.8	18–22 [7]	2016	PBr	dextral reverse	Multifault, multiple fault types	≥6**	180

Notes
CI = continental interior; PB = plate boundary; PBr = plate boundary region,
*f/s is foreshock
** Depending on the definition of single faults, onshore-offshore connections, and connectivity the fault number may range up to 21 (Litchfield et al., 2018)
[1] Rizza et al., 2011
[2] Petersen and Wesnousky, 1994
[3] Matmon et al., 2006
[4] Fletcher et al., 2014
[5] Hornblow et al., 2014
[6] Amos et al. (2013) reported approximately 0.7 mm year^{-1} for the adjacent Little Lake Fault (LLF). The Eastern Little Lake Fault that ruptured in 2019 had no known prior surface rupture, so constraint is only that it must be less than LLF
[7] Litchfield et al., 2014

distribution plot developed by Mason and Little (2006) (their figure 4) is relatively uniform along strike with an average of 5.3 ± 1.6 m over the 110 km, fault parallel, length, but, clearly, the total rupture length is longer than 110 km with 3.7 and 4.8 m displacements observed at the ends of the mapped rupture. Bartholomew et al. (2014) map the offshore Awatere Fault for a further 6 km into Cook Strait, although there is complexity at the end of the trace with the Vernon Fault. Bartholomew et al. (2014) confirm there was no 1848 rupture on the Vernon Fault or nearby Cloudy Bay Fault in the region of the northeast termination of the Awatere Fault in the nearshore area.

Considering the large (4.8 m) dextral displacement on the BPF at Barefell Pass mapped by Mason and Little (2006) on the western part of the 1848 rupture, we may presume the rupture extended somewhat further south on the BPF toward the Clarence Fault. The BPF has not been mapped in detail in the steep terrain especially in the Guide River, but Mason (2004) suggests that the dip of the BPF is about 50°, much less than the steeper dips along much of the Awatere Fault. We speculate that the BPF was originally a Mesozoic structure formed during Pahau terrane accretion but has now been reactivated in the Cenozoic and acts as a potential linking structure between the Clarence and Awatere Faults. The BPF may act to facilitate multifault rupture in much the same way as the Papatea Fault in the 2016 Kaikōura earthquake fault ruptures, although it did not do so in association with the 1848 earthquake.

The slip distribution of the 1848 rupture published by Mason and Little (2006) has no marked variation in slip distribution making it difficult to infer unilateral or bilateral rupture. However, the isoseismal map developed by Grapes and Downes (1997) is elongate toward the northeast, suggesting rupture started in the southwest on the BPF and propagated northeast onto the Awatere Fault. We do acknowledge that except along the east coast of the South Island there is little control in the southwest direction of the felt intensities, so early in New Zealand's written historical record. A more symmetric isoseismal shape could be expected if the earthquake had been strongly felt in Christchurch, but this is not the case.

5.2. 1855 M 8.2 Wairarapa Fault (Figure 8B)

The largest earthquake in New Zealand's written history (since about 1840) occurred in southern North Island on the Wairarapa Fault just 7 years after the Awatere Fault rupture in 1848. Although largely a North Island earthquake, the fault lies within Pahau Terrane bedrock close to and parallel with the eastern margin of the Esk Head melange (Figure 1). In terms of surface rupture complexity there is evidence from both the northern and southern ends of the rupture for bifurcation, and partial rupture of additional faults. The isoseismal contours that can be attributed to the 1855 earthquake are approximately equidimensional around the probable surface rupture extent (Grapes and Downes, 1997; Downes, 2005) and maximum surface displacement of 18 m dextral (Rodgers and Little, 2006) is approximately along the middle-southern section of the fault. A bilateral rupture is therefore most likely in 1855. The probable northern termination of 1855 surface rupture has been assessed from earthquake geology studies (Schermer et al., 2004) showing a likely rupture of the 7 km long Dreyers Road Fault and partial rupture of the southern section of the Alfredton Fault (Figure 1 and Table 2). At the southern end, the on-land surface rupture occurred in a slip partitioned fashion with reverse faulting on the Wharekahau Thrust south of the Mukamuka Fault along the eastern shore of Cape Palliser and with a strike-slip strand to the west, within the Remutaka Range (Little et al., 2009). This inland strike-slip trace may reach the south coast in the vicinity of the Orongorongo River mouth. Offshore, Barnes (2005) has mapped the probable extent as two strands extending up to 40 km south of Cape Palliser (Figure 1). The southern extent is thus close to the northern extension of the Needles Fault that ruptured in the 2016 Kaikōura earthquake. Undoubtedly, the 1855 surface faulting was more complex than can be mapped from geological studies more than 100 years after the event, but no data are available that suggests multifault rupture of the complexity observed during the Kaikōura earthquake. The main feature of complexity is at the north end where the rupture stepped approximately 7 km eastward from the Wairarapa Fault to the Alfredton Fault via normal displacement on the Dreyers Road Fault.

5.3. 1888 M 7.1 Hope Fault (Figure 8D)

This event on the Hope Fault is important in both New Zealand and globally as it was arguably the first time that horizontal displacement was documented (McKay, 1890). The extent of surface faulting was determined from field studies and distinctions were made between probable primary surface rupture and secondary cracking and fissuring (McKay, 1890). More recently, changes in strike along the length of the fault or geometric steps in the surface geometry have been identified and used as the basis to define possible geometric rupture segments (Cowan, 1991; Langridge and Berryman, 2005; Langridge et al., 2013; Khajavi et al., 2016). The Hope Fault has thus been divided into geometric segments. Khavaji et al. (2016), using paleoseismic and tree ring dating techniques to determine the western end of the 1888 rupture, demonstrated that the rupture broke through the approximately 12° change in strike that defines the geometric segment boundary between the Hope River segment and the Hurunui segment. This is largely the extent of complexity manifest in the 1888 surface rupture other than local splays and complexity due to topographic effects. The eastern end

of the 1888 rupture was at the approximately 8 km right step in the Hope Fault at the Hanmer basin (McKay, 1890; Wood et al., 1994; Khavaji et al., 2016) (Figure 1 and Table 2).

5.4. 1929 M 7.1 Poulter Fault (Figure 8E)

The March 9, 1929 earthquake was the largest earthquake in New Zealand since the 1888 event on the Hope Fault. The epicentral area is in a remote mountainous area of central South Island (Figure 1) and much of the attention in the aftermath of the earthquake was on landslides including the large Falling Mountain landslide. Only limited field reconnaissance was undertaken (Speight, 1933) and this earthquake was quickly overshadowed by the M 7.8 Buller earthquake that occurred just a few months later. Hancox et al. (1997) later refined the landslide distributions associated with large earthquakes in New Zealand and Doser et al. (1999) refined the focal mechanism and epicentre of the 1929 earthquake. This focussed field studies on the possible location of the causative fault associated with the 1929 earthquake (Berryman and Villamor, 2004). A newly defined active fault, the Poulter Fault, was thus identified, about 70 years after the event (Berryman and Villamor, 2004). No significant rupture complexity was identified, but the passage of time and the mountainous region precluded detailed surface rupture mapping. We can, however, be confident that the rupture was not so complex as to include the nearby Kakapo or Hope Faults (Figure 1 and Table 2).

5.5. Summary findings from historic surface fault rupture in the MTD

Prior to the 2016 earthquake, the prior surface rupturing earthquakes in the MTD occurred 93–174 years ago. In some cases, field studies soon after the earthquakes revealed principal elements of the surface faulting that occurred (e.g., McKay, 1890; Speight, 1933), but, in several cases, the determination of the extent of surface faulting was undertaken much more recently (e.g., Berryman and Villamor, 2004; Schermer et al., 2004; Mason & Little, 2006) and much of the detail is likely to have been lost. Nevertheless, multifault rupture of the complexity observed in 2016 can be discounted in the earlier events. There were ruptures that extended onto another geometric section of the fault in the case of the 1888 Hope Fault earthquake, and similarly onto the end of the Alfredton Fault in 1855 (although the Alfredton Fault can also be considered an additional geometric section of the Wairarapa Fault).

Collett et al. (2019) and Ghisetti (2021) discuss some variation in the timing and extent of deformation and geomorphic development in the MTD related to evolution of the MFS, but the bulk deformation of bedrock appears less marked than the differences in rupture complexity between 2016 and earlier events. At most, multifault rupture in earlier events consisted of two faults, but in 2016 at least 6 different faults ruptured (and could be more depending on definitions of faults and rupture connectivity). Therefore, we consider the 2016 to be fundamentally different to what occurred in the prior period covering almost 200 years (see Table 2).

6. Complex ruptures internationally (Figure 9)

The complex rupture and associated surface faulting in the 2016 Kaikōura event joins a growing list of recognised 'complex' events. The recognition of complexity in part results from increasingly robust monitoring networks, earth observation techniques, and computational advancements to integrate diverse datasets (e.g., Howell et al., 2019). Most recently Ross et al. (2019) and Plesch et al. (2020) documented the remarkable complexity associated with the 2019 Ridgecrest earthquake and its Mw 6.4 foreshock. While this complexity in surface fault rupture seems remarkable it is most unlikely that earthquakes are becoming more complex with time, but rather the technology to map and identify complexity is improving rapidly.

As long ago as the 1957 Mw 8 Gobi-Altai earthquake, the surface rupture pattern indicated the source must have included essentially simultaneous rupture of several faults judging by the separation distance between surface ruptures with diverse rupture characteristics (Florensov and Solonenko, 1965; Kurushin et al., 1997; Prentice et al., 2002; Choi et al., 2012) (Figure 9A). Similar complexity also occurred in the 1992 Mw 7.1 Landers earthquake (Rockwell et al., 2000) (Figure 9B) although the faults were all arranged along-strike with relay connections. The 1999 Mw 7.4 İzmit earthquake in Turkey and the Mw 7.1 Düzce earthquake triggered event three months later were relatively simple strike-slip ruptures with extensional step-overs and secondary normal faults (Barka et al., 2002) (Figure 9C). The 2002 Mw 7.9 Denali Fault rupture actually began with rupture of a subsidiary reverse fault at the northwestern end of the rupture, propagated onto the Denali Fault and then terminated on a subsidiary splay at the southeastern end (Dreger et al., 2004) (Figure 9D). This again is an example of an end-on cascade but it was predominantly a simple rupture' of the Denal Fault. The 2010 Mw7.2 El Mayor-Cucapah earthquake was associated with rupture of parallel strands of a single fault with a long history of displacement on strands with variable kinematics (Fletcher et al., 2014) (Figure 9E). The 2010 Mw7.1 Darfield earthquake (Quigley et al., 2010) (Figure 9F) is a New Zealand example that presents as a relatively simple surface fault rupture with small step-overs, but, in the subsurface, as many as six separate structures ruptured based on geodetic and seismological data (Beavan et al., 2012) to remind us that surface ruptures provide one insight into earthquake rupture complexity but rarely

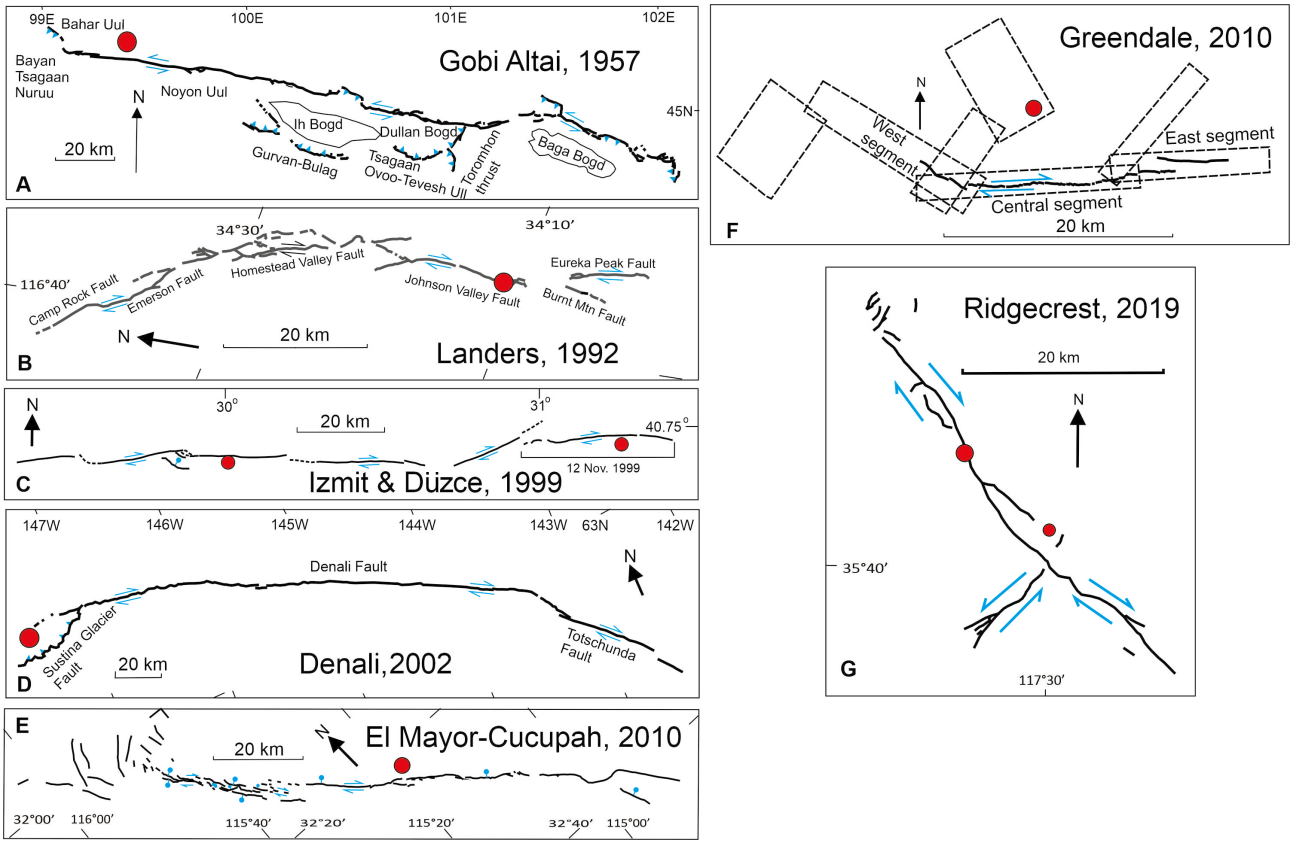

Figure 9. Surface fault rupture maps from complex and multifault rupture examples globally. Summarised from published research referenced in the text. Subsurface faults associated with the 2010 Greendale Fault rupture is from Beavan et al. (2012). Red circles are the epicentres of the mainshocks.

will this be so simple at seismogenic depth. This raises the question of the appropriateness in using surface fault ruptures as a basis for source modelling in seismic hazard studies. The 2019 Mw7.1 Ridgecrest earthquake (Ross et al., 2019; Plesch et al., 2020) (Figure 9G) is not strictly a single event but rather a foreshock and mainshock or a sequence with two earthquakes occurring 34 h apart. The surface ruptures occurred in an orthogonal pattern corresponding to very strong orthogonal bedrock faulting. Each subset of surface faulting was relatively simple.

In Table 2, we summarise aspects of some international and New Zealand examples of surface fault rupture with variable surface rupture complexity. The tectonic environments in which these earthquakes occurred, ranging from continental interior in the case of the 1957 Gobi-Altai earthquake to plate boundary in the case of the 1999 İzmit and Düzce earthquakes on the North Anatolian Fault in Turkey and the 2002 Denali earthquake. Earthquakes in plate boundary regions include those in the MTD, Landers, El Mayor-Cucupah, Darfield, and the 2016 Kaikōura event. Fault slip rates vary in these examples from <0.1–17 mm year^{-1}. There is a reasonable correlation between slip rate and complexity with low slip rate corresponding to the most complex events (but this is not the case for the 2016 Kaikōura event). Similarly, more complexity is observed for continental interior and edges of plate boundary regions than for plate boundary faults that are characterised by fast slip rates and large total displacement. Structural complexity, exemplified by the setting of the Ridgecrest pair of earthquakes and transition zones in plate boundary settings such as Kaikōura are characterised with multifault ruptures (Plesch et al., 2020). Although at different scales there are some similarities in the surface rupture pattern in the 1848 Awatere and 2002 Denali events with a subsidiary rupture on reverse faults prior to propagation onto the main strike-slip fault. In general, examples of strike-slip ruptures (Landers, İzmit, Awatere, Hope and the Jordan-Kekerengu-Needles component of the Kaikōura rupture), no matter the tectonic environment, often display similar levels of rupture complexity—generally single fault but often including multisegment rupture. Moreover, the subsurface complexity inferred from seismicity and geodetic data for the 2010 Darfield and 2019 Ridgecrest have some similarity illustrating strong control from bedrock structure on the rupture pattern.

Complexity as a result of fault mechanism is also highly variable and reverse fault ruptures are especially complex (Rubin, 1996). We do not review the complexity related to reverse fault ruptures here because they are not so relevant to the MFS which is the main objective of this paper. However, we note the propensity for multifault and surface rupture complexity described by Rubin (1996). Similarly, where faults and/or structural heterogeneities are oblique to the stress field then ruptures often partition into vertical and horizontal components (e.g., Barth et al., 2012; Toda et al., 2016) with up to several kilometres separation of strands. This is a feature of the southern section of the Wairarapa Fault rupture in 1855 (Figure 8B), but it was an essentially single fault rupture.

7. Prospects for future rupture complexity in the Marlborough tectonic domain

Geological structure and geological history of the region has preconditioned the brittle crust of the Marlborough domain to potential complex fault rupture and rupture propagation because of interconnections on a myriad of faults associated with deformation episodes over the past 100 Ma. These episodes include imbricate reverse faults formed in a Gondwana subduction zone when the Pahau Terrane rocks were deposited and lithified (Ring et al., 2019), both low and high angle normal faults associated with Gondwana breakup and opening of the Tasman Sea (Crampton et al., 2003) and reverse and then strike-slip faulting along with vertical axis rotation as the present-day plate boundary was established (Randall et al., 2011). As a result of block rotation and reorientation of plate motions, many of the older faults in the region are adequately oriented (Sibson, 1990) to be reactivated as linking structures between the now-dominant strike-slip faults of the Marlborough Fault System (MFS). The probable shallow dip of many of the older structures in the middle crust and the utilisation of these shallow-dipping faults in the establishment of the MFS in the past 2–5 Ma enhances the likelihood of connections at or about the base of the brittle crust at approximately 15 km depth in Marlborough.

Therefore, the complexity of the surface ruptures and the way in which the 2016 earthquake ruptures propagated is not perhaps surprising. What is surprising is that surface ruptures of four other historic large earthquakes in the Marlborough tectonic domain (including the 1855 rupture in southern North Island in a similar tectonic setting) do not appear to have been nearly as complex. We acknowledge that our understanding of rupture complexity in these older 19th and 20th century will not be as complete as was possible in the 2016 earthquake, but widespread multifault rupture can be ruled out despite the similar tectonic setting and presence of similar bedrock structure.

Great complexity in 2016 may therefore be a feature of that particular part of the MTD, and in particular the area involving the complex transition of slip between the Hope Fault and the Jordan-Kekerengu-Needles Fault. While the Hope Fault was not significantly involved in the 2016 earthquake, slip did transition from south of the Hope Fault into the MTD via closely spaced diverse structures that are possibly linked at depth. Nowhere else in the MTD do such high strain rates and closely spaced, diverse structures exist (Morris et al., 2022). Howell and Clark (2022) and Langridge et al. (2022), using data from Holocene marine along the Kaikōura coast and the Papatea Fault, respectively, linked to nearby on-fault data, have investigated evidence for prior multifault or clustered earthquake episodes in the area. Although the data cannot distinguish between one large rupture or several ruptures separated by days-years, there are indications for earlier episodes of multifault or clustered earthquake activity involving largely offshore upper plate faults that drive coastal uplift, possibly coupled with Kekerengu Fault rupture. At the Humps Fault, Brough et al. (2021) investigated the paleoseismic history and found that the mean recurrence interval is 1.8–3.4 ka and indicated that the Humps Fault may be linked with '2016 Kaikōura type' ruptures every approximately 2 ka, while the Hope and Kekerengu Faults have recurrence intervals of 200–400 years (Hatem et al., 2019; Morris et al., 2022).

The complex rupture in 2016 (Figure 1) has impacted the seismic hazard community with calls for wider adoption of multifault ruptures in fault networks (e.g., Page, 2021). We suggest that the 2016 Kaikōura multifault ruptures may, in general, be repeatable in that same area of the Marlborough tectonic domain but do not seem to be characteristic of the northeast or central parts of the MTD, although several prior events have at least partial rupture of a second geometric section or there are subsidiary splay faults involved. In the southwest of the MTD where the MFS approaches the southeast-dipping Alpine Fault they are interacting with the Alpine Fault at depth effectively reducing their downdip and the faults splay into a horsetail arrangement (Vermeer et al., 2021). Therefore, multifault ruptures may be expected in future large earthquakes at the western ends of the Hope, Clarence, and Awatere Faults. Overall, caution is suggested so that the uniqueness of the Kaikōura event in 2016 does not drive hazard assessment methodology to infer complex multifault rupture in all future large earthquakes in this region, and globally. Consideration of geological structure and history may usefully be incorporated into seismic hazard methodology to evaluate when and where multifault source models are appropriate.

8. Conclusion

The 2016 Kaikōura earthquake occurred in the transition zone between westward subduction of the Pacific plate

at the HSZ in the North Island and oblique continental collision along the transpressional Alpine Fault to the southwest. The event was complex both seismologically and geologically, but not dissimilar to other large historical events globally. The complexity observed in Marlborough in 2016 in part results from increasingly robust monitoring networks, earth observation techniques, and computational advancements to integrate diverse datasets.

The pattern and number of faults that ruptured was surprising to many. However, consideration of the past geological history of the region (recognising numerous tectonic overprints with diverse faulting styles) coupled with the realisation that the current strike slip faults are immature in their structural development provide insights into the reasons for multifault rupture occurrence. Connecting structures at seismogenic depth between the major active faults that ruptured in 2016 are likely. This connectivity is particularly likely in the nexus around the transfer of slip from the Hope Fault to the Jordan-Kekerengu-Needles Fault. The assertion of likely shallower fault dip at depth of many of the currently active faults in the region is supported by the crustal seismic mapping identifying this geometry for the Wairarapa Fault that hosted the Mw 8.2 1855 earthquake that was accompanied by up to 18 m of dextral strike-slip displacement at maximum.

Examination of other historic surface rupturing earthquakes in the Marlborough tectonic domain do not show the same level of multifault rupture although partial rupture of a secondary geometric section and some splay faulting appears common. We propose that the particular part of the tectonic domain where a large part of the plate boundary deformation transfers from the Hope Fault to the Jordan-Kekerengu-Needles Fault, with acute changes in fault geometry and closely spaced faults with diverse rupture characteristics, may be particularly likely to host multifault complex ruptures. Our assessment indicates the 2016 multifault rupture should not reorient seismic hazard methodology toward highly multifault rupture as the norm rather than the exception.

Acknowledgements

It is with pleasure that we present this contribution to the Aykut Barka memorial volume. His contribution, leadership, and respect live on in New Zealand and globally. We thank Gülsen Uçarkuş, special editor, in supporting this submission. We thank Robert Langridge for insightful review comments on an early draft of this manuscript, and useful comments from an anonymous journal reviewer.

References

Amos CB, Brownlee SJ, Rood DH, Fisher GB, Bürgmann R et al. (2013). Chronology of tectonic, geomorphic, and volcanic interactions and the tempo of fault slip near Little Lake, California. Bulletin Seismological Society of America 125 (7-8): 1187-1202.

Ando R, Kaneko Y (2018). Dynamic rupture simulation reproduces spontaneous multi-fault rupture and arrest during the 2016 Mw 7.9 Kaikōura earthquake. Geophysical Research Letters 45 (23): 12,875-12,883.

Bailleul J, Chanier F, Ferrière J, Robin C, Nicol A et al. (2013). Neogene evolution of lower trench-slope basins and wedge development in the central Hikurangi subduction margin, New Zealand. Tectonophysics 591, 152-174.

Barnes PM, Nicol A, Harrison T (2002). Late Cenozoic evolution and earthquake potential of an active listric thrust complex above the Hikurangi subduction zone, New Zealand. Geological Society of America Bulletin 114 (11): 1379-1405.

Barnes PM (2005). The southern end of the Wairarapa Fault, and surrounding structures in Cook Strait. In: The 1855 Wairarapa Earthquake Symposium: 150 Years of Thinking About Magnitude 8+ Earthquakes and Seismic Hazard in New Zealand. Proceedings Volume (pp. 66-71).

Barka A, Akyuz HS, Altunel E, Sunal G, Cakir Z et al. (2002). The surface rupture and slip distribution of the 17 August 1999 Izmit earthquake (M 7.4): North Anatolian fault. Bulletin of the Seismological Society of America 92 (1): 43-60.

Barth NC, Toy VG, Langridge RM, Norris RJ (2012). Scale dependence of oblique plate-boundary partitioning: New insights from LiDAR, central Alpine fault, New Zealand. Lithosphere 4 (5): 435-448.

Bartholomew TD, Little TA, Clark KJ, Van Dissen R, Barnes PM (2014). Kinematics and paleoseismology of the Vernon Fault, Marlborough Fault System, New Zealand: Implications for contractional fault bend deformation, earthquake triggering, and the record of Hikurangi subduction earthquakes. Tectonics 33 (7): 1201-1218.

Batt GE, Baldwin SL, Cottam MA, Fitzgerald PG, Brandon MT et al. (2004). Cenozoic plate boundary evolution in the South Island of New Zealand: New thermochronological constraints. Tectonics 23 (4): TC4001. https://doi.org/10.1029/2003TC001527.

Beavan J, Darby D (2005). Fault slip in the 1855 Wairarapa earthquake based on new and reassessed vertical motion observations: Did slip occur on the subduction interface. In: The 1855 Wairarapa Earthquake Symposium: 150 Years of Thinking About Magnitude 8+ Earthquakes and Seismic Hazard in New Zealand. Proceedings Volume (pp. 31-41).

Beavan J, Motagh M, Fielding EJ, Donnelly N, Collett D (2012). Fault slip models of the 2010–2011 Canterbury, New Zealand, earthquakes from geodetic data and observations of postseismic ground deformation. New Zealand Journal of Geology and Geophysics 55 (3): 207-221.

Berryman K., Villamor P (2004). Surface rupture of the Poulter Fault in the 1929 March 9 Arthur's Pass earthquake, and redefinition of the Kakapo Fault, New Zealand. New Zealand Journal of Geology and Geophysics 47 (2): 341-351.

Bishop DG (1972). Progressive metamorphism from prehnite-pumpellyite to greenschist facies in the Dansey Pass area, Otago, New Zealand. Geological Society of America Bulletin 83 (11): 3177-3198.

Bradshaw JD (1989). Cretaceous geotectonic patterns in the New Zealand region. Tectonics 8 (4): 803-820.

Brough T, Nicol A, Stahl T, Pettinga JR, Van Dissen R et al. (2021). Paleoseismicity of the western Humps fault on the Emu Plain, North Canterbury, New Zealand. New Zealand Journal of Geology and Geophysics, https://doi.org/10.1080/00288306.2021.1986727.

Cashman SM, Kelsey HM, Erdman CF, Cutten HN, Berryman KR (1992). Strain partitioning between structural domains in the forearc of the Hikurangi subduction zone, New Zealand. Tectonics 11 (2): 242-257.

Cesca S, Zhang Y, Mouslopoulou V, Wang R, Saul J et al. (2017). Complex rupture process of the Mw 7.8, 2016, Kaikōura earthquake, New Zealand, and its aftershock sequence. Earth and Planetary Science Letters 478: 110-120.

Chamberlain CJ, Frank WB, Lanza F, Townend J, Warren-Smith E (2021). Illuminating the Pre-, Co-, and Post-Seismic Phases of the 2016 M7. 8 Kaikōura Earthquake With 10 Years of Seismicity. Journal of Geophysical Research: Solid Earth 126 (8): e2021JB022304.

Choi JH, Jin K, Enkhbayar D, Davvasambuu B, Bayasgalan A, Kim YS (2012). Rupture propagation inferred from damage patterns, slip distribution, and segmentation of the 1957 MW8. 1 Gobi-Altay earthquake rupture along the Bogd fault, Mongolia. Journal of Geophysical Research: Solid Earth 117 (B12401): https://doi.org/10.1029/2011JB008676.

Collett CM, Duvall AR, Flowers RM, Tucker GE, Upton P (2019). The timing and style of oblique deformation within New Zealand's Kaikōura Ranges and Marlborough Fault System based on low-temperature thermochronology. Tectonics 38 (4): 1250-1272.

Clark KJ, Nissen EK, Howarth JD, Hamling IJ, Mountjoy JJ et al. (2017). Highly variable coastal deformation in the 2016 Mw7.8 Kaikōura earthquake reflects rupture complexity along a transpressional plate boundary. Earth and Planetary Science Letters 474: 334-344.

Cowan HA (1991). The north Canterbury earthquake of September 1, 1888. Journal of the Royal Society of New Zealand 21 (1): 1-12.

Cowan H, Nicol A. Tonkin P (1996). A comparison of historical and paleoseismicity in a newly formed fault zone and a mature fault zone, North Canterbury, New Zealand. Journal of Geophysical Research: Solid Earth 101 (B3): 6021-6036.

Cox SC, Sutherland R (2007). Regional geological framework of South Island, New Zealand, and its significance for understanding the active plate boundary. In, A continental plate boundary: tectonics at South Island, New Zealand. AGU Monograph 175: 19-46.

Crampton J, Laird M, Nicol A, Townsend D, Van Dissen R (2003). Palinspastic reconstructions of southeastern Marlborough, New Zealand, for mid-Cretaceous-Eocene times. New Zealand Journal of Geology and Geophysics 46 (2): 153-175.

Christensen NI, Mooney WD (1995). Seismic velocity structure and composition of the continental crust: a global view. Journal of Geophysical Research, 100, 9761–9788.

Darby DJ, Beanland S (1992). Possible source models for the 1855 Wairarapa earthquake, New Zealand. Journal of Geophysical Research: Solid Earth 97 (B9): 12375-12389.

Diederichs A, Nissen EK, Lajoie LJ, Langridge RM, Malireddi SR et al. (2019). Unusual kinematics of the Papatea fault (2016 Kaikōura earthquake) suggest anelastic rupture. Science Advances 5 (10): p.eaax5703.

Doser DI; Webb TH; Maunder DE (1999). Source parameters of large historical (1918-1962) earthquakes, South Island, New Zealand. Geophysical Journal International 139: 769-794.

Downes GL (2005). The 1855 January 23 M8+ Wairarapa earthquake - what contemporary accounts tell us about it. In: The 1855 Wairarapa Earthquake Symposium: 150 Years of Thinking About Magnitude 8+ Earthquakes and Seismic Hazard in New Zealand. Proceedings Volume (pp. 1-10).

Dreger DS, Oglesby DD, Harris R, Ratchkovski N, Hansen R (2004). Kinematic and dynamic rupture models of the November 3, 2002 Mw7. 9 Denali, Alaska, earthquake. Geophysical Research Letters 31 (4): L04605. https://doi.org/10.1029/2003GL018333.

Eberhart-Phillips D, Bannister S (2010). 3-D imaging of Marlborough, New Zealand, subducted plate and strike-slip fault systems. Geophysical Journal International 182 (1): 73-96.

Eberhart-Phillips D, Bannister S, Ellis S (2014). Imaging P and S attenuation in the termination region of the Hikurangi subduction zone, New Zealand. Geophysical Journal International 198 (1): 516-536.

Eberhart-Phillips D, Ellis S, Lanza F, Bannister S (2021a). Heterogeneous material properties as inferred from seismic attenuation-influenced multiple fault rupture and ductile creep of the Kaikōura Mw 7.8 earthquake, New Zealand. Geophysical Journal International 227 (2): 1204-1227.

Eberhart-Phillips D, Bannister S, Reyners M, Ellis S, Lanza F (2021b). New Zealand Wide model 2.3 Qs and Qp models for New Zealand, updated for Kaikōura (Qnzwide2.3) [Data set]. Zenodo. https://doi.org/10.5281/zenodo 5098356

Edbrooke SW, Heron DW, Forsyth PJ, Jongens R (compilers) (2014). Online geological map of New Zealand 1:1 000 000: https://data.gns.cri.nz/geology/ [last accessed 1 May, 2020]

Ellis S, Van Dissen R, Eberhart-Phillips D, Reyners M, Dolan JF et al. (2017). Detecting hazardous New Zealand faults at depth using seismic velocity gradients. Earth and Planetary Science Letters 463: 333-343.

Fletcher JM, Teran OJ, Rockwell TK, Oskin ME, Hudnut KW et al. (2014). Assembly of a large earthquake from a complex fault system: Surface rupture kinematics of the 4 April 2010 El Mayor–Cucapah (Mexico) Mw 7.2 earthquake. Geosphere 10 (4): 797-827.

Florensov NA, Solonenko VP (Eds.). (1965). The Gobi-Altay Earthquake. Jerusalem: Israel Program for Scientific Translations, pp 424.

Forsyth PJ, Barrell DJA, Jongens R (compilers) (2008). Geology of the Christchurch area: scale 1:250,000. Lower Hutt: GNS Science. Institute of Geological & Nuclear Sciences 1:250,000 geological map 16. 67 p. + 1 folded map.

Ghisetti FC (2021). Map-view restorations of the South Island, New Zealand: a reappraisal of the last 10 Myr of evolution of the Alpine and Wairau faults. New Zealand Journal of Geology and Geophysics 64: 1-26. https://doi.org/10.1080/00288306.2021.1878243.

Goldberg DE, Melgar D, Sahakian VJ, Thomas AM, Xu X et al. (2020). Complex rupture of an immature fault zone: A simultaneous kinematic model of the 2019 Ridgecrest, CA earthquakes. Geophysical Research Letters 47 (3): e2019GL086382.

Grapes R, Downes G (1997). The 1855 Wairarapa, New Zealand, earthquake. Bulletin of the New Zealand Society for Earthquake Engineering, 30 (4): 271-368.

Hamling IJ, Hreinsdóttir S, Clark K, Elliott J, Liang C et al. (2017). Complex multi-fault rupture during the 2016 Mw 7.8 Kaikōura earthquake, New Zealand, Science 356: 6334. https://doi.org/10.1126/science. eeam7194

Hamling IJ (2019). A review of the 2016 Kaikōura earthquake: insights from the first 3 years. Journal of the Royal Society of New Zealand, https://doi.org/10.1080/03036758.2019.170104.

Hancox GT, Perrin ND, Dellow GD (1997). Earthquake-induced landsliding in New Zealand and implications for MM intensity and seismic hazard assessment. Earthquake Commission Project Report 95/196.

Hatem AE, Dolan JF, Zinke RW, Van Dissen RJ, McGuire CM et al. (2019). A 2000 yr paleoearthquake record along the Conway segment of the Hope fault: Implications for patterns of earthquake occurrence in northern South Island and southern North Island, New Zealand. Bulletin of the Seismological Society of America 109 (6): 2216-2239.

Henrys S, Wech A, Sutherland R, Stern T, Savage M et al. (2013). SAHKE geophysical transect reveals crustal and subduction zone structure at the southern Hikurangi margin, New Zealand. Geochemistry, Geophysics, Geosystems 14 (7): 2063-2083.

Howard M, Nicol A, Campbell J, Pettinga JR (2005). Holocene paleoearthquakes on the strike-slip Porters Pass fault, Canterbury, New Zealand. New Zealand Journal of Geology and Geophysics 48 (1): 59-74.

Howarth JD, Cochran UA, Langridge RM, Clark K, Fitzsimons SJ et al. (2018). Past large earthquakes on the Alpine Fault: paleoseismological progress and future directions. New Zealand Journal of Geology and Geophysics 61 (3): 309-328.

Howell A, Nissen E, Stahl T, Clark K, Kearse J et al. (2019). 3D surface displacements during the 2016 Mw7.8 Kaikōura earthquake (New Zealand) from photogrammetry-derived point clouds. Journal of Geophysical Research, https://doi.org/10.1029/2019JB018739.

Howell A, Clark KJ (2022). Late Holocene coseismic uplift of the Kaikōura coast, New Zealand. Geosphere 4, https://doi.org/10.1130/GES02479.1.

Hudnut KW, Borsa A, Glennie C, Minster JB (2002). High-resolution topography along surface rupture of the October 16, 1999 Hector Mine earthquake (Mw7.1) from airborne laser swath mapping. Bulletin of the Seismological Society of America 92: 1570–1576.

Hutchison AA, Böse M, Manighetti I (2020). Improving early estimates of large earthquake's final fault lengths and magnitudes leveraging source fault structural maturity information. Geophysical Research Letters 47 (14): e2020GL087539.

Kaiser A, Balfour N, Fry B, Holden C, Litchfield N et al. (2017). The 2016 Kaikōura, New Zealand, earthquake: preliminary seismological report. Seismological Research Letters 88 (3): 727-739.

Kearse J, Little TA, Van Dissen RJ, Barnes PM, Langridge R et al. (2018). Onshore to Offshore Ground-Surface and Seabed Rupture of the Jordan–Kekerengu–Needles Fault Network during the 2016 Mw 7.8 Kaikōura Earthquake, New Zealand. Bulletin of the Seismological Society of America 108 (B3): 1573-1595.

Khajavi N, Langridge RM, Quigley MC, Smart C, Rezanejad A et al. (2016). Late Holocene rupture behavior and earthquake chronology on the Hope fault, New Zealand. Bulletin of the Seismological Society of America 128 (11-12): 1736-1761.

Kurushin A, Bayasgalan A, lziybat, MO, Enkhtuvshin B, Molnar P et al. (1997). The surface rupture of the 1957 Gobi-Altay, Mongolia, earthquake. Geological Society of America, Special Paper, 320, 143 pp.

Lamarche G, Beanland S, Ravens J (1995). Deformation style and history of the Eketahuna region, Hikurangi forearc, New Zealand, from shallow seismic reflection data. New Zealand Journal of Geology and Geophysics 38 (1): 105-115.

Landis CA, Campbell HJ, Begg JG, Mildenhall DC, Paterson AM et al. (2008). The Waipounamu Erosion Surface: questioning the antiquity of the New Zealand land surface and terrestrial fauna and flora. Geological Magazine 145 (2): 173-197.

Langridge RM, Berryman KR (2005). Morphology and slip rate of the Hurunui section of the Hope fault, South Island, New Zealand. New Zealand Journal of Geology and Geophysics 48 (1): 43–57. https://doi.org/10.1080/00288306.2005.9515097

Langridge RM, Almond PC, Duncan RP (2013). Timing of late Holocene paleoearthquakes on the Hurunui segment of the Hope fault: Implications for plate boundary strain release through South Island, New Zealand. Geological Society of America Bulletin 125 (5–6): 756–775. https://doi.org/10.1130/B30674.1

Langridge RM, Rowland J, Villamor P, Mountjoy JJ, Madugo C et al. (2018). Coseismic rupture and slip on the Papatea fault and its role in the 2016 Kaikōura, New Zealand, earthquake, Bulletin of the Seismological Society of America, https://doi.org/10.1785/0120170336.

Langridge RM, Clark KJ, Almond P, Baize S, Howell A et al. (2022). Late Holocene earthquakes on the Papatea Fault and its role in past earthquake cycles, Marlborough, New Zealand. New Zealand Journal of Geology and Geophysics, 1-25.

Lanza F, Chamberlain CJ, Jacobs K, Warren-Smith E, Godfrey HJ et al. (2019). Crustal fault connectivity of the Mw 7.8 2016 Kaikōura earthquake constrained by aftershock relocations. Geophysical Research Letters 46 (12): 6487-6496.

Lensen GJ (1962). Sheet 16 Kaikōura. Geological Map of New Zealand scale 1:250,000, Dept. of Scientific & Industrial Research, Wellington, New Zealand.

Litchfield NJ, Campbell JK, Nicol A (2003). Recognition of active reverse faults and folds in North Canterbury, New Zealand, using structural mapping and geomorphic analysis. New Zealand Journal of Geology and Geophysics 46 (4): 563-579.

Litchfield NJ, Van Dissen R, Sutherland R, Barnes PM, Cox SC et al. (2014). A model of active faulting in New Zealand. New Zealand Journal of Geology and Geophysics 57 (1): 32-56.

Litchfield NJ, Villamor P, Van Dissen RJ, Nicol A, Barnes PM et al. (2018). Surface rupture of multiple crustal faults in the 2016 M w 7.8 Kaikōura, New Zealand, earthquake. Bulletin of the Seismological Society of America 108 (B3): 1496-1520.

Little TA, Jones A (1998). Seven million years of strike-slip and related off-fault deformation, northeastern Marlborough fault system, South Island, New Zealand. Tectonics 17 (2): 285-302.

Little TA, Van Dissen R, Schermer E, Carne R (2009). Late Holocene surface ruptures on the southern Wairarapa fault, New Zealand: Link between earthquakes and the uplifting of beach ridges on a rocky coast. Lithosphere 1 (1): 4-28.

Little TA, Van Dissen R, Kearse J, Norton K, Benson A et al. (2018). Kekerengu fault, New Zealand: Timing and size of Late Holocene surface ruptures. Bulletin of the Seismological Society of America 108 (B3): 1556-1572.

Long DT, Cox SC, Bannister S, Gerstenberger MC, Okaya D (2003). Upper crustal structure beneath the eastern Southern Alps and the Mackenzie Basin, New Zealand, derived from seismic reflection data. New Zealand Journal of Geology and Geophysics 46 (1): 21-39.

Mason DP (2004). Neotectonics and paleoseismicity of a major junction between two strands of the Awatere Fault, South Island, New Zealand. MSc thesis Victoria University of Wellington, New Zealand.

Mason DP, Little TA (2006). Refined slip distribution and moment magnitude of the 1848 Marlborough earthquake, Awatere Fault, New Zealand. New Zealand Journal of Geology and Geophysics 49 (3): 375-382.

Matmon A, Schwartz DP, Haeussler PJ, Finkel R, Lienkaemper JJ et al. (2006). Denali fault slip rates and Holocene–late Pleistocene kinematics of central Alaska. Geology 34 (8): 645-648.

McArthur AD, Claussmann B, Bailleul J, Clare A, McCaffrey WD (2020). Variation in syn-subduction sedimentation patterns from inner to outer portions of deep-water fold and thrust belts: examples from the Hikurangi subduction margin of New Zealand. Geological Society of London, Special Publications 490 (1): 285-310.

McGill SF, Rubin CM (1999). Surficial slip distribution on the central Emerson fault during the June 28, 1992, Landers earthquake, California. Journal of Geophysical Research: Solid Earth 104 (B3): 4811-4833.

McKay A (1890). On the Earthquakes of September 1888 in the Amuri and Marlborough Districts of the South Island: New Zealand Geological Survey Report of Geological Explorations 20: 1–16.

Milliner CWD, Sammis C, Allam AA, Dolan JF, Hollingsworth J et al. (2016). Resolving fine-scale heterogeneity of co-seismic slip and the relation to fault structure. Nature, Scientific Reports 6 (1): 1-9.

Morris P, Little T, Van Dissen R, Hemphill-Haley M, Kearse J et al. (2022). A revised paleoseismological record of late Holocene ruptures on the Kekerengu Fault following the 2016 Kaikōura earthquake. New Zealand Journal of Geology and Geophysics, https://doi.org/10.1080/00288306.2022.2059766.

Mortimer N, Rattenbury MS, King PR, Bland KJ, Barrell DJA et al. (2014). High-level stratigraphic scheme for New Zealand rocks. New Zealand Journal of Geology and Geophysics 57 (4): 402-419. https://doi.org/10.1080/00288306.2014.946062.

Mouslopoulou V, Saltogianni V, Nicol A, Oncken O, Begg J et al. (2019). Breaking a subduction-termination from top to bottom: The large 2016 Kaikōura Earthquake, New Zealand. Earth and Planetary Science Letters 506: 221-230.

Nicol A, Khajavi N, Pettinga J, Fenton C, Stahl T et al. (2018). Preliminary geometry and kinematics of surface ruptures in the epicentral area during the 2016 Mw 7.8 Kaikōura, New Zealand, earthquake, Bulletin of the Seismological Society of America, https://doi.org/ 10.1785/0120170329.

Nicol A, Begg J, Saltogianni V, Mouslopoulou V, Oncken O, Howell A. (2022). Uplift and fault slip during the 2016 Kaikōura Earthquake and Late Quaternary, Kaikōura Peninsula, New Zealand. New Zealand Journal of Geology and Geophysics, https://doi.org/10.1080/00288306.2021.2021955.

Page MT (2021). More fault connectivity is needed in seismic hazard analysis. Bulletin of the Seismological Society of America 111 (1): 391-397.

Petersen MD, Wesnousky SG (1994). Fault slip rates and earthquake histories for active faults in southern California. Bulletin of the Seismological Society of America 84 (5): 1608-1649.

Pettinga JR, Yetton MD, Van Dissen RJ, Downes G (2001). Earthquake source identification and characterisation for the Canterbury region, South Island, New Zealand. Bulletin of the New Zealand Society for Earthquake Engineering 34 (4): 282-317.

Plesch A, Shaw JH, Ross ZE. Hauksson E (2020). Detailed 3D fault representations for the 2019 Ridgecrest, California, earthquake sequence. Bulletin of the Seismological Society of America 110 (4): 1818-1831.

Prentice CS, Kendrick K, Berryman K, Bayasgalan A, Ritz JF, Spencer JQ (2002). Prehistoric ruptures of the Gurvan Bulag fault, Gobi Altay, Mongolia. Journal of Geophysical Research: Solid Earth 107 (B12): ESE-1.

Quigley M, Van Dissen, R, Litchfield N, Villamor P, Duffy B et al. (2012). Surface rupture during the 2010 Mw 7.1 Darfield (Canterbury) earthquake: implications for fault rupture dynamics and seismic-hazard analysis. Geology 40: 55–58.

Rait G, Chanier F, Waters DW. (1991). Landward-and seaward-directed thrusting accompanying the onset of subduction beneath New Zealand. Geology 19 (3): 230-233.

Randall K, Lamb S, Mac Niocaill C (2011). Large tectonic rotations in a wide zone of Neogene distributed dextral shear, northeastern South Island, New Zealand. Tectonophysics 509 (3-4): 165-180.

Rattenbury MS, Townsend DB, Johnston MR (comps) (2006). Geology of the Kaikoura area: scale 1:250,000 geological map. Lower Hutt: GNS Science. Institute of Geological & Nuclear Sciences 1:250,000 geological map 13. 70 p. + 1 folded map.

Ring U, Mortimer N, Deckert H (2019). Critical-wedge theory and the Mesozoic accretionary wedge of New Zealand. Journal of Structural Geology 122: 1-10.

Rizza M, Ritz JF, Braucher R, Vassallo R, Prentice C et al. (2011). Slip rate and slip magnitudes of past earthquakes along the Bogd left-lateral strike-slip fault (Mongolia). Geophysical Journal International 186 (3): 897-927.

Rockwell TK, Lindvall S, Herzberg M, Murbach D, Dawson T et al. (2000). Paleoseismology of the Johnson Valley, Kickapoo, and Homestead Valley faults: Clustering of earthquakes in the eastern California shear zone. Bulletin of the Seismological Society of America 90 (5): 1200-1236.

Rodgers DW, Little TA (2006). World's largest coseismic strike-slip offset: The 1855 rupture of the Wairarapa Fault, New Zealand, and implications for displacement/length scaling of continental earthquakes. Journal of Geophysical Research: Solid Earth 111 B12408, https://doi.org/10.1029/2005JB004065.

Ross ZE, Idini B, Jia Z, Stephenson OL, Zhong M et al. (2019). Hierarchical interlocked orthogonal faulting in the 2019 Ridgecrest earthquake sequence. Science 366 (6463): 346-351.

Rubin CM (1996). Systematic underestimation of earthquake magnitudes from large intracontinental reverse faults: Historical ruptures break across segment boundaries. Geology 24 (11): 989-992.

Schermer ER, Van Dissen R, Berryman KR, Kelsey, HM, Cashman SM (2004). Active faults, paleoseismology, and historical fault rupture in northern Wairarapa, North Island, New Zealand. New Zealand Journal of Geology and Geophysics 47 (1): 101-122.

Seebeck H, Van Dissen R, Litchfield N, Barnes P, Nicol A et al. (2021). New Zealand Community Fault Model – version 1.0. Lower Hutt (NZ): GNS Science. 97pp. (GNS Science report; 2021/57). https://doi.org/10.21420/GA7S-BS61.

Sibson RH (1990). Rupture nucleation on unfavourably oriented faults. Bulletin of the Seismological Society of America 80 (6): 1580-1604.

Speight R (1933). The Arthur's Pass earthquake of 9th March, 1929. New Zealand Journal of Science and Technology 15 (3): 173-182.

Stahl T (2014). Active Tectonics and Geomorphology of the central South Island, New Zealand: Earthquake Hazards of Reverse Faults. PhD thesis, University Canterbury, Christchurch, New Zealand.

Stirling MW, McVerry G, Gerstenberger M, Litchfield N, Van Dissen, R et al. (2012). National seismic hazard model for New Zealand: 2010 update. Bulletin of the Seismological Society of America 102: 1514–1542.

Stirling MW, Litchfield NJ, Villamor P, Van Dissen RJ, Nicol A et al. (2017). The Mw 7.8 2016 Kaikōura earthquake: Surface fault rupture and seismic hazard context. Bulletin of the New Zealand Society for Earthquake Engineering 50: 73-84.

Toda S, Kaneda H, Okada S, Ishimura D, Mildon ZK (2016). Slip-partitioned surface ruptures for the Mw 7.0 16 April 2016 Kumamoto, Japan, earthquake. Earth, Planets and Space, 68 (1): 1-11.

Ulrich T, Gabriel AA, Ampuero JP, Xu W (2019). Dynamic viability of the 2016 Mw 7.8 Kaikoura earthquake cascade on weak crustal faults. Nature Communications 10 (1): 1-16.

Van Dissen R, Yeats RS (1991). Hope fault, Jordan thrust, and uplift of the seaward Kaikoura Range, New Zealand. Geology 19 (4): 393-396.

Wallace LM, Beavan J, McCaffrey R, Berryman K, Denys P (2007). Balancing the plate motion budget in the South Island, New Zealand using GPS, geological and seismological data. Geophysical Journal International 168 (1): 332-352.

Wesnousky SG (1988). Seismological and structural evolution of strike-slip faults. Nature 335 (6188): 340-343.

Williams CA, Eberhart-Phillips D, Bannister S, Barker DH, Henrys S et al. (2013). Revised interface geometry for the Hikurangi subduction zone, New Zealand. Seismological Research Letters 84: 1066–1073.

Williams JN, Barrell DJ, Stirling MW, Sauer KM, Duke GC, Hao KX (2018). Surface rupture of the Hundalee fault during the 2016 M w 7.8 Kaikōura earthquake. Bulletin of the Seismological Society of America 108 (B3): 1540-1555.

Wood R, Pettinga JR, Bannister S, Lamarche G, McMorran T (1994). Structure of the Hanmer strike-slip basin, Hope fault, New Zealand. Geological Society of America Bulletin 106: 1459-1473.

Xu W, Feng G, Meng L, Zhang A, Ampuero JP et al. (2018). Transpressional rupture cascade of the 2016 Mw 7.8 Kaikoura earthquake, New Zealand. Journal of Geophysical Research: Solid Earth 123 (3): 2396-2409.

Zinke R, Hollingsworth J, Dolan JF, Van Dissen R (2019). Three-dimensional surface deformation in the 2016 Mw 7.8 Kaikōura, New Zealand, earthquake from optical image correlation: Implications for strain localization and long-term evolution of the Pacific-Australian plate boundary. Geochemistry, Geophysics, Geosystems 20 (3): 1609-1628.